Available online at www.sciencedirect.com

ScienceDirect

Geochimica et Cosmochimica Acta 247 (2019) 220–242

Geochimica et Cosmochimica Acta

www.elsevier.com/locate/gca

Snow algae drive productivity and weathering at volcanic rock-hosted glaciers

Jeff R. Havig [a,*], Trinity L. Hamilton [b,c]

[a] Dept. of Earth Sciences, University of Minnesota, Minneapolis, MN 55455, USA
[b] Dept. of Plant and Microbial Biology, University of Minnesota, St. Paul, MN 55108, USA
[c] BioTechnology Institute, University of Minnesota, St. Paul, MN 55108, USA

Received 6 August 2018; accepted in revised form 18 December 2018; available online 27 December 2018

Abstract

Earth has experienced periodic local to global glaciation for nearly 3 billion years, providing supra- and subglacial environments for colonization by microbial communities. A number of studies have reported on the role of microbial communities in glacial ecosystems including their influence on element cycling and weathering, but there is a paucity data on volcanic rock-hosted glacial ecosystems. Glaciers on stratovolcanoes in the Pacific Northwest override silica-rich rocks which represent analogues to an early Martian cryosphere. On these glaciers, blooms of photosynthetic snow algae support supraglacial microbial communities as has been observed on snowfields, glaciers, and ice sheets. In subglacial environments of volcanic rock-hosted glacial systems, weathering is driven, at least in part, by carbonic acid, suggesting a link between supraglacial carbon sources and subglacial heterotrophic microbial communities. Here, we report inorganic carbon assimilation and microbial community composition on glaciers across three stratovolcanoes ranging in composition from dacitic to mafic in the Pacific Northwest of the United States to begin to constrain the role of supraglacial primary productivity in subglacial weather processes. These data, coupled to contextual carbon and nitrogen isotope analyses of biomass and aqueous geochemistry, indicate snow algae drive light dependent carbon uptake across supraglacial and periglacial environments. Furthermore, snow algae microbial communities are supported by fixed nitrogen predominantly from deposition via precipitation. Our data highlight intense cycling of carbon and nitrogen driven by supraglacial microbial communities that feeds subglacial microbial communities which in turn may drive weathering processes. These results further underscore the role of glacial ecosystems in global biogeochemical cycling, especially during past global glaciations. Finally, these results lend support for glaciers as refugia for biodiversity on Earth and potentially on other bodies such as Mars where evidence exists for widespread and long-lived cryosphere including glaciers and ice sheets.

Keywords: Snow algae; Carbon isotopes; Weathering; Supraglacial; Periglacial; Subglacial; Carbon uptake; Pacific Northwest; Alpine

1. INTRODUCTION

Glaciers are present on six of the seven continents, with an estimated 15 million square kilometers of the Earth's land surface currently covered by ice sheets, ice caps, and glaciers. Alpine glaciers represent important sources of water for watersheds supporting agricultural and drinking water sources through summer dry periods in the Pacific Northwest (PNW), with glacial melt contributions of 41–73% for streams and rivers sourced from Mt. Hood, OR (Nolin et al., 2010). PNW glaciers have experienced rapid retreat over the last century (Lillquist and Walker, 2006), with predictions that 77% of PNW glaciers will not survive

* Corresponding author at: 116 Church Street SE, 150 Tate Hall, Minneapolis, MN 55455-0231, USA.
E-mail address: jhavig@umn.edu (J.R. Havig).

https://doi.org/10.1016/j.gca.2018.12.024
0016-7037/

in the current and predicted climate (Pelto, 2010), making the study of these endangered systems imperative before they are gone.

Snow and ice surfaces associated with glaciers are teeming with life, harboring dynamic microbial communities supported by light-dependent carbon fixation by snow algae. Snow algae are cosmopolitan, having been described globally in alpine regions and on icefields including North America (e.g., Takeuchi, 2013; Hamilton and Havig, 2017, 2018), Greenland (e.g., Uetake et al., 2010; Yallop et al., 2012; Lutz et al., 2014), Iceland (e.g., Lutz et al., 2015), Svalbard (e.g., Lutz et al., 2017a), Europe (e.g., Remias et al., 2009; Lutz et al., 2017a), the Russian Arctic (e.g., Hisakawa et al., 2015; Tanaka et al., 2016); the Himalaya (e.g., Yoshimura et al., 1997), Japan (e.g., Terashima et al., 2017), South America (e.g., Takeuchi and Kohshima, 2004), and Antarctica (e.g., Fujii et al., 2010; Grzesiak et al., 2015). Most of what is known about snow algae communities has been learned from studies centered on glaciers and snowfields located on sedimentary or metamorphic bedrock, but little is known about snow algae systems hosted in volcanic bedrock (Hamilton and Havig, 2017). Recent work has quantified primary productivity as predominantly phototrophically mediated, and demonstrated inorganic carbon limitation of primary productivity by snow algae communities on PNW glaciers (Hamilton and Havig, 2017, 2018) suggesting increasing productivity with increasing atmospheric CO_2 concentrations. However, microbial community composition distribution, primary productivity rates, and nitrogen source determination across supraglacial and periglacial surfaces on volcanic bedrock hosted glaciers in the PNW remain poorly constrained.

Subglacial systems are the weathering regions where most breakdown of rock and liberation of anions and cations from bedrock and sediments occurs (Sharp et al., 1999; Foght et al., 2004; Mitchell et al., 2013; Boyd et al., 2014; Rutledge et al., 2018). Supraglacial input of organic carbon is known to be delivered to subglacial microbial communities (Hodson et al., 2005; Hamilton et al., 2013), and can drive weathering in volcanic subglacial systems through heterotrophic breakdown of organic material, generating CO_2 which when dissolved in water generates carbonic acid (H_2CO_3). Carbonic acid is a primary driver of weathering in volcanic hosted glacial systems, resulting in the release of cations and dissolved silica (Rutledge et al., 2018). A better understanding of microbial community composition and elemental cycling on and through glacial systems is required to constrain biological activity for the Earth system during global and regional glaciation events going as far back as 2.9 Ga (Young et al., 1998; Royer et al., 2004; Kopp et al., 2005; Melezhik, 2006; Fairchild and Kennedy, 2007; Rasmussen et al., 2013; Gumsley et al., 2017). Furthermore, glacial systems hosted in volcanic systems as harbors and potentially refugia for microbial communities may have implications for the surface of Mars, which may have been glaciated for at least 3 billion years (Kargel and Strom, 1992; Head et al., 2005; Madeleine et al., 2009; Bernhardt et al., 2013; Ramirez and Craddock, 2018).

Here we report carbon uptake values for 15 different sites across three stratovolcanoes in the Cascade Range of Washington and Oregon (Fig. 1). These uptake values are coupled to microbial community composition determinations, natural abundance $\delta^{13}C$ and $\delta^{15}N$ values for microbial communities and nearby contextual samples, and associated aqueous geochemistry. To address these questions, a suite of samples were collected across three glacial systems in the PNW including pigment-colored snow, dirty snow with no visible pigment, and sediments in outwash channels, ponded water on glacial surfaces, or in moraine-dammed lakes at the bases of glaciers (Fig. 1). Using these samples, microbial community compositions, carbon uptake rates, and C and N content and isotopic values were determined. Furthermore, contextual samples including allochthonous organic material and autochthonous aqueous geochemistry were collected to better constrain elemental cycling (e.g., C and N) and movement (e.g., silica, cations, and trace elements) through the glacial systems.

2. METHODS

2.1. Sample site selection

Sites were selected to represent a wide range of microbial community biomass, based on previous work (Hamilton et al., 2013; Hamilton and Havig, 2017, 2018). Glaciers were selected to represent volcanic rocks with a range of silica content, from more silicic (Mt. Hood, andesitic to dacitic) to more mafic (North and Middle Sisters, andesitic basalt to basaltic). On these glaciers sampling sites were selected to capture a range of supraglacial to subglacial to peri-glacial environments. Supraglacial environments included pigment-colored snow, sediment-rich snow, and sediment and pigment-poor (dirty) snow. Subglacial environments were represented by mid-glacier outwash channels and end of glacier outflow channels with sustained flow through the night (during sampling, all supraglacial surface melt ended after nightfall, with local temperatures dropping below 0 °C and surface runoff halting). Outwash channels on Collier Glacier and Eliot Glacier sustained higher-conductivity and sediment-ladened flow throughout the night and were sampled multiple times throughout the day as well as in the morning prior to initiation of melt to capture effects of supraglacial vs. subglacial input. Periglacial environments were represented by ponded water, end-moraine-dammed lakes, and distal springs that emerged well below glaciers and end moraines. Glaciers sampled included Gotchen Glacier on Mt. Adams, WA; Eliot and Palmer Glaciers on Mt. Hood; and Collier and Diller Glaciers on the North and Middle Sisters (Fig. 1).

To characterize the C and N isotopic values of snow algae microbial communities and differentiate between allochthonous and autochthonous organic material, contextual samples from on and near the glaciers was collected. This included insects found on glacial surfaces, plants growing on sediments on and next to glacial sampling sites, and forest soils near glaciers. Insects included bugs, beetles, bees, wasps, spiders, flies, and ice worms (Collier only occurrence). Plants included evergreen tree needles (Moun-

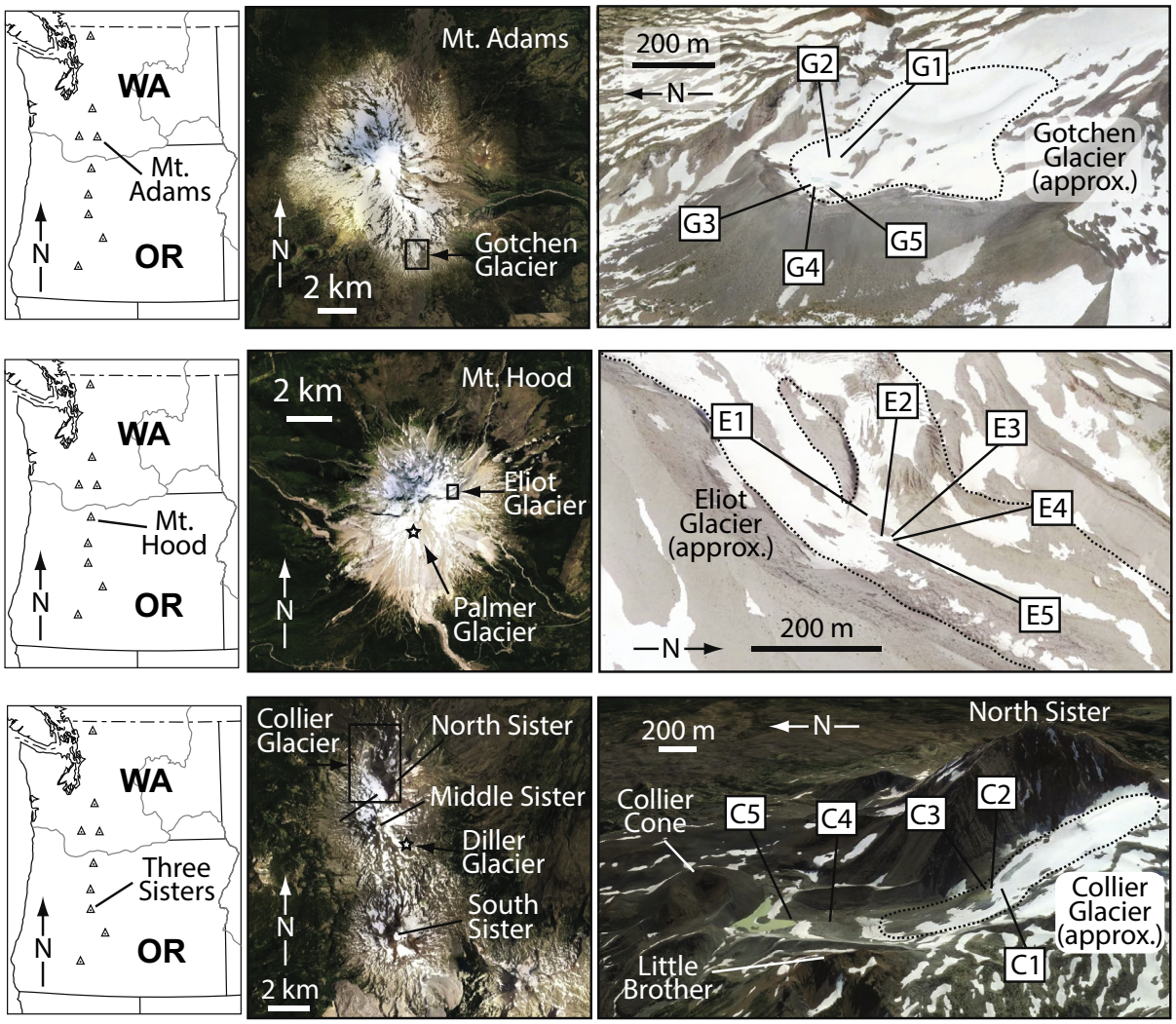

Fig. 1. Maps and sampling locations. Top left: location of Mt. Adams. Top center: location of Gotchen Glacier. Black box shows location of Gotchen Glacier and arrow indicates direction of view for image at top right. Top right: sampling locations at Gotchen Glacier. Dotted line shows approximate boundary of Gotchen Glacier. Middle left: location of Mt. Hood. Middle center: location of Eliot Glacier (open box) and Palmer Glacier (open star). Black box shows location of Eliot Glacier sampling area and arrow indicates direction of view for image at middle right. Middle right: sampling locations at Eliot Glacier. Dotted line shows approximate boundary of Eliot Glacier. Bottom left: location of Three Sisters. Bottom center: location of Collier Glacier on North Sister (open box) and Diller Glacier (open star). Black box shows location of Collier Glacier and arrow indicates direction of view for image at bottom right. Bottom right: sampling locations at Collier Glacier. Dotted line shows approximate boundary of Collier Glacier. All images courtesy Google Earth.

tain Hemlock and White Pine), grasses, broad-leafed plants (lupine, penstemon, monkey flower, and aster), a succulent, and mosses and lichens. Forest soils were collected from the first occurrence of established trees with developed soils underneath at the closest approach to the glaciers. Plants and insects were selected based on observed occurrences associated with supraglacial environments.

2.2. Sampling

Water samples were filtered through 0.2 μm polyethersulfone syringe filters and distributed into bottles for later geochemical analysis as described previously (Hamilton and Havig, 2017). Samples for induced coupled plasma optical emission spectroscopy (ICP-OES) and induced coupled plasma mass spectrometry (ICP-MS) were filtered into a 15 mL centrifuge tubes that had been acid washed (soaked in 10% trace element clean HNO_3 for three days, triple rinsed with 18.2 MΩ/cm deionized water), acidified (200 μL of concentrated OmniTrace Ultra™ concentrated nitric acid (EMD Millipore, Billerica, MA)), and kept on ice/refrigerated at 4 °C in the dark until analysis. ICP-OES analysis for Ca, Na, K, Mg, P, and Si, and ICP-MS analysis for Al, Ti, Mn, and Fe was conducted at the Analytical Geochemistry Laboratory in the Department of Earth Sciences at the University of Minnesota.

Samples for dissolved inorganic carbon (DIC) analysis were filtered into a gas-tight syringe and then injected into Labco Exetainers® (Labco Limited, Lampeter, UK) pre-flushed with He, with excess He removed following introduction of 8 mL of filtered sample with minimal agitation. Samples were stored inverted until and on ice/refrigerated at 4 °C until returned to the lab, where 1 mL of concentrated H_3PO_4 was added and the samples shipped to the Stable Isotope Facility (SIF) at the University of California, Davis for analysis. DIC analysis for concentration and ^{13}C isotopic signal using a GasBench II system interfaced to a Delta V Plus isotope ratio mass spectrometer (IR-MS) (Thermo Scientific, Bremen, Germany) with raw delta values converted to final using laboratory standards (lithium carbonate, $\delta^{13}C = -46.6‰$ and a deep seawater, $\delta^{13}C = +0.8‰$) calibrated against standards NBS-19 and L-SVEC. Samples for dissolved organic carbon (DOC) analysis were filtered through a 0.2 μm polyethersulfone syringe filter that had been flushed with ~30 mL of sample and then ~40 mL put into a 50 mL centrifuge tube and then immediately flash-frozen on dry ice and kept frozen and in the dark until analysis at the SIF. DOC analysis for concentration and ^{13}C isotopic signal were carried out using O.I. Analytical Model 1030 TOC Analyzer (O.I. Analytical, College Station, TX) interfaced to a PDZ Europa 20-20 isotope ratio mass spectrometer (Sercon Ltd., Cheshire, UK) utilizing a GD-100 Gas Trap Interface (Graden Instruments) for concentration and isotope ratio determination with raw delta values converted to final using laboratory standards (KHP and cane sucrose) calibrated against USGS-40, USGS-41, and IAEA-600.

Fixed nitrogen compounds, including NO_3^-, NO_2^-, and $NH_4(T)$ ($NH_4(T) = NH_3 + NH_4^+$), were determined at the time of sampling via a Hach DR 1900 spectrophotometer. Temperature and pH were measured in situ using an Extech pH meter and probe (Nashua, NH). A subset of samples at Collier Glacier had pH determined via four-stage litmus paper (Thermo Fisher Scientific, USA) following failure of the pH meter in the field, and are indicated in Tables 3a and 3b.

2.3. CO_2 photoassimilation and natural abundance

Inorganic carbon uptake was assessed *in situ* using a microcosm-based approach through the addition of $NaH^{13}CO_3$. In selected sampling sites, samples were collected from the surface using a pre-sterilized spatula, placed into a clean container, and if in snow allowed to melt to a slush-slurry. An equal volume of snow slurry (~10 mL) or sediment (~5 g) was then transferred into each well of a sterile six well tray and the lid placed over the tray. Assays were initiated by addition of $NaH^{13}CO_3$ (Cambridge Isotope Laboratories, Inc., Andover MA) (100 μM final concentration). Each sample was placed into one six well tray per site.

At each site, we assessed the potential for photoautotrophic (light) and chemoautotrophic (dark) $NaH^{13}CO_3$ uptake. To assess CO_2 assimilation in the dark, six well trays ($n = 1$ per site) were amended with $NaH^{13}CO_3$ and completely wrapped in aluminum foil. All reported values of DIC uptake (carbon fixation rates) reflect the difference in uptake between the labeled and unlabeled assays. Following incubation time ($t \approx 2$ h), incubation trays were flash frozen on dry ice and kept frozen until processed.

Following return to the lab, incubation samples were rinsed with 1 M HCl to remove any carbonate minerals and any residual ^{13}C DIC label, triple rinsed with 18.2 MΩ/cm deionized water and dried (8 h, 60 °C). Of the six wells, two each were combined to generate three replicates for each treatment (light and dark). Natural abundance C and N contextual samples were collected in either 15 mL centrifuge tubes or 2 mL cryovials, flash-frozen on dry ice, and kept frozen until processed for analysis. Natural abundance samples were dried (8 h, 60 °C). Natural abundance samples and incubation samples were ground and homogenized using a clean mortar and pestle (silica sand and 80% ethanol slurry ground between samples, then mortar and pestle rinsed with ethanol followed by 18.2 MΩ/cm deionized water and dried).

Carbon and nitrogen concentration and isotopic signal were determined as described previously (Hamilton and Havig, 2017, 2018). In short, samples were weighed and placed into tin boats, sealed, and analyzed via a Costech Instruments Elemental Analyzer (EA) periphery connected to a Thermo Scientific Delta V Advantage Isotope Ratio Mass Spectrometer (IR-MS) at the Stable Isotope Geochemistry Lab in the Department of Geology at the University of Cincinnati. Linearity corrections were made using NIST Standard 2710, and $\delta^{13}C$ values were calibrated using reference standards USGS-40 and USGS-41 and checked with a laboratory standard (glycine). Total uptake of DIC was calculated using DIC numbers determined for the source water (described above). All stable isotope results are given in delta formation expressed as per mil (‰). Carbon stable isotopes are calculated as:

$$\delta^{13}C = \left[\left((R_a)_{sample}/(R_a)_{standard}\right) - 1\right] \times 10^3 \quad (1)$$

where R_a is the $^{13}C/^{12}C$ ratio of the sample or standard, and are reported versus the Vienna Pee Dee Belemnite (VPDB) standard. Natural abundance samples also had $\delta^{15}N$ values determined as described for $\delta^{13}C$, reported versus atmospheric air.

2.4. DNA extraction and quantification

Total DNA was extracted from triplicate samples of biomass (~250 mg each) using a DNeasy PowerSoil Kit (Qiagen) according to the manufacturer's instructions and quantified using a Qubit dsDNA HS Assay kit and a Qubit 3.0 Fluorometer (Life Technologies). Equal volumes of each extraction were pooled into a single sample and submitted to the University of Minnesota Genomics Center for amplicon sequencing. As negative DNA extraction controls, DNA was extracted from the 0.2 μm polyethersulfone syringe filter used for the field blank water sample (described above) and from the 18.2 MΩ/cm water used for the field blank. No DNA was detected in the negative controls and sequencing of these extracts failed to generate amplicons (see below for amplicon sequencing details).

2.5. Sequence analysis

Amplicons were sequenced using MiSeq Illumina 2 × 300 bp chemistry with the primers 515Ff and 806rB targeting V4 hypervariable region of bacterial and archaeal 16S SSU rRNA gene sequences (Caporaso et al., 2012; Apprill et al., 2015) and the primers E572F and E1009 targeting the V9 hypervariable region of eukaryotic 18S SSU rRNA gene sequences (Comeau et al., 2011) using a dual-indexing approach (Gohl et al., 2016). Each sample was sequenced once.

Post sequence processing was performed within the mothur (ver. 1.37.6) sequence analysis platform (Schloss et al., 2009) following the MiSeq SOP (Kozich et al., 2013) as described previously (Hamilton and Havig, 2017). On average, 16S rRNA amplicon libraries contained 53,708 reads and 18S rRNA amplicon libraries contained 103,221 reads (SOM Fig. 1). Unique sequences were aligned against a SILVA-based reference alignment and classified using a Bayesian classifier within mothur against the Silva (v132) reference taxonomy. Chimeras were identified in the aligned sequences using UCHIME (Edgar et al., 2011) with the Silva SEED database (v132) and removed from further analyses. Singletons were removed using the remove rare function within mothur. Following removal of chimeras and singletons, operational taxonomic units (OTUs) were assigned to all classified 16S rRNA sequences at 97.0% using the average-neighbor algorithm and to all classified 18S rRNA sequences at 98.0% using the average-neighbor algorithm. Previous studies indicate 97% sequence identity for 18S rRNA sequences is too conservative for estimating the diversity of microbial eukaryotes (Stoeck et al., 2010). At this level of similarity, taxonomic assignment can be made to the genus level (Maritz et al., 2017). A total of 5400 18S rRNA OTUs and 6218 16S rRNA OTUs were recovered. Within sample diversity (alpha diversity) were calculated using using MicrobiomeAnalyst (Dhariwal et al., 2017). Observed OTUs, Chao1 and Shannon diversity index were calculated to examine community richness and evenness. Heatmaps were calculated and visualized using ampvis ((v. 1.27.021; Albertsen et al., 2015) and Phylosq (McMurdie and Holmes, 2013). Pairwise differences between communities were calculated within mothur to form distance matrices that were used to generate non-metric multidimensional scaling (NMDS) ordination which was plotted using R (ver. 3.4.4; R Core Team, 2017). Spearman correlation analyses of the most abundant OTUs and physicochemical parameters was performed using vegan (ver 2.5-3; Oksanen et al., 2018) in R (ver. 3.4.4). Sequence data including raw reads, quality scores and mapping data have been deposited in the NCBI Sequence Read Archive (SRA) database with the BioProject number PRJNA483479 (SOM Table 1).

3. RESULTS

3.1. Community composition and diversity

The majority of 18S rRNA sequences recovered from the three study areas and from all sampling sites were affiliated with unicellular green algae, predominantly from Chlorophyceae (primarily Chlamydomonales) (Figs. 2–4; SOM Fig. 2) and Trebouxiophyceae (primarily Prasiolales). We also observed abundant sequences affiliated with Glissomonadida (flagellate gliding bacteriovores found in soils and fresh water) and Cercozoa (heterotrophs/bacterivores found in soil and fresh and marine water environments) across most samples sites. Sequences affiliated with Intramacronucleata (ciliated protists) were abundant in sediment samples from Eliot, Collier, and Gotchen Glaciers. We also recovered small numbers of OTUs affiliated with fungi including Microbotryomycetes and Pezizomycotina (filamentous ascomycetes that include most lichenized fungi). In general, 18S rRNA diversity in snow algae samples spanned a larger range than sediment samples while sediment samples were slightly more diverse than snow algae samples (SOM Fig. 3). For the snow algae samples, the observed and estimated number of OTUs (Chao1) were highest in samples from Collier and Eliot Glacier and lowest in samples from Gotchen Glacier. These samples also had higher values of Shannon diversity compared to Gotchen Glacier snow algae samples. The highest observed and expected number of OTUs in the sediment samples were recovered from two samples from Collier Glacier (C2 and C3), E5 from Eliot Glacier and G4 from Gotchen Glacier. Shannon diversity was also highest in these samples. Analyses of beta diversity among the 18S rRNA libraries indicates that snow algae samples are more related to one another than the sediment samples (SOM Fig. 4).

In the 16S rRNA amplicon libraries, sequences affiliated with Sphingobacteriia, Betaproteobacteriales and Alphaproteobacteria, Cytophagia, and Actinobacteria, were abundant across all samples (Figs. 2–4; SOM Fig. 5). Sequences affiliated with OPB35 soil group were also abundant, particularly in supraglacial snow algae samples (SOM Fig. 5). In contrast to the 18S rRNA diversity, 16S rRNA diversity in snow algae samples varied much less whereas a large range in variability was observed in the diversity of 16S rRNA sequences in the sediment samples (SOM Fig. 6). Among sediment samples, C2 from Collier Glacier and G4 and G5 from Gotchen Glacier were most diverse in terms of Chao1 and Shannon diversity metrics whereas C3, C4, C5 and G3 exhibited the lowest levels of diversity in the data set. Similar to the 18S rRNA libraries, beta diversity between the 16S rRNA visualized with NMDS indicates the snow algae communities are more closely related to one another than the sediment microbial communities (SOM Fig. 7).

3.2. $\delta^{13}C$ and $\delta^{15}N$ natural abundance analyses

$\delta^{13}C$ values for snow algae communities ($n = 15$) fell between −28.61 and −24.0‰, and $\delta^{15}N$ values fell between −7.90 and 0.41‰ (Table 1). Contextual samples were collected from all glacial areas and included soils ($n = 4$), grasses ($n = 9$), evergreen tree needles (white pine and western hemlock, $n = 6$), broadleaf plants ($n = 3$, aster and monkeyflower), lupines ($n = 2$), succulents ($n = 1$), mosses and lichens ($n = 5$), insects ($n = 15$, including bugs, flies, bees, beetles, spiders, and wasps), and ice worms ($n = 1$,

Table 1
Carbon and nitrogen analysis results for biomass and context samples.

Sample ID	Sample Description	Glacier Site	C uptake ID	Total C %	S. D.	$\delta^{13}C$ ‰	S. D.	Total N %	S. D.	$\delta^{15}N$ ‰	S. D.
Snow Algae Microbial Community Biomass											
160729C**	Red Algae	Gotchen	G1	5.94		−24.19		0.328		−5.59	
160729D	Orange Algae	Gotchen	G2	6.81		−28.61		0.512	0.154	−4.21	0.16
160729E	Lake seds	Gotchen	G5	*0.03*		−26.78		*0.002*		bdl	
160729F	snow edge seds	Gotchen	G3	1.90		−26.44		0.162		0.41	
160729G	dirty snow	Gotchen	G4	0.56	0.02	−25.93	0.32	0.041	0.000	−1.13	
160730A	snow algae	Eliot	E1	0.35	0.01	−26.95	0.43	0.024	0.001	−6.49	
160730B	Glacial Outwash	Eliot	E5	*0.01*		−26.42		*0.002*		bdl	
160730C	foamy seds	Eliot	E4	0.64		−27.01		0.068		−5.81	
160730D	snow edge seds	Eliot	E2	1.54	0.10	−28.23	0.00	0.116	0.008	bdl	
160730E	dirty snow	Eliot		0.61		−27.61		0.062		−6.23	
160731I	mat seds	Eliot	E3	0.06	0.03	−26.02		*0.007*	*0.004*	bdl	
160802A	Diller South Beach	Diller		0.08		−25.92		0.007		bdl	
160802B	Dirty Orange Snow	Diller		0.63		−27.33	0.27	0.049	0.006	−3.82	
160806B	Collier's Spa	Collier	C5	0.09		−25.31		0.006		bdl	
160806C	Collier Bubbler	Collier	C4	0.02	0.01	−24.97	0.49	*bdl*		bdl	
160806D	Collier Base Outwash	Collier		*0.00*		*−25.10*		*0.001*		bdl	
160806G	snow algae	Collier	C1	0.48	0.08	−24.02	0.12	0.025	0.010	−4.75	
160806H	edge seds	Collier	C2	0.07	0.03	−27.15		*0.007*	*0.005*	bdl	
160806I	runoff time series site	Collier	C3	0.03		−27.05		*bdl*		bdl	
JRH160806I	dried tan biofilm	Collier		0.12	0.02	−26.76		0.014	0.004	bdl	
160807N	Upper Runoff 5	Collier		0.07		−25.58		0.006		bdl	
150620A	Top of Timberline Algae	Palmer		4.01	0.04	−24.29	0.03	0.209	0.001	−5.88	0.04
150620B*	Salty Palmer Algae	Palmer		3.29	0.02	−25.87	0.04	0.156	0.000	−6.20	0.22
150621G*	El pollo rojo loco algae	Gotchen		6.14	0.26	−24.09	0.02	0.410	0.016	−3.76	0.17
150621E*	Hellroaring algae	Gotchen		29.66	1.08	−26.20	0.61	1.475	0.062	−4.09	0.08
150622I*	Eliot Beach Algae	Eliot		0.98	0.01	−26.85	0.07	0.093	0.002	−4.54	0.41
150622K	Eliot supraglacial floc	Eliot		0.44	0.00	−26.88	0.08	0.054	0.001	−7.90	0.21
156025P*	Collier algae	Collier		0.97	0.00	−26.54	0.00	0.064	0.001	−4.11	0.04
Context samples											
150624N	Ice Worms	Collier		31.42	0.22	−25.90	0.12	4.249	0.023	−1.80	0.02
150621 E2	Forest Soil	Gotchen		0.61	0.02	−25.65	0.08	0.045	0.000	2.57	0.44
JRH160729L	Forest Soil	Gotchen		2.07		−26.56		0.144		1.14	
JRH160802E	Forest Soil	Diller		4.28		−24.75		0.183		2.23	
JRH160807A	Forest Soil	Collier		2.82		−25.84		0.214		2.56	
JRH160806A	White Pine Needles	Collier		48.60		−27.37		1.209		−8.91	
JRH160802D	White Pine Needles	Diller		48.75		−26.35		1.456		−8.90	
JRH160729M	White Pine Needles	Gotchen		46.44		−26.22		1.918		−2.90	
JRH160729K	White Pine Needles	Gotchen		48.32		−28.40		*2.081*		−4.38	
JRH160731L	White Pine Needles	Eliot		48.30	0.49	−26.66	0.55	1.410	0.210	1.76	0.90
JRH160731M	Mountain Hemlock Needles	Eliot		47.37	1.85	−22.90	0.26	1.476	0.097	−0.25	
JRH160806E	Money Flower	Collier		43.99	0.56	−29.64	1.25	1.863		−5.65	

(*continued on next page*)

Table 1 (*continued*)

Sample ID	Sample Description	Glacier Site	C uptake ID	Total C %	S. D.	$\delta^{13}C$ ‰	S. D.	Total N %	S. D.	$\delta^{15}N$ ‰	S. D.
JRH160806F	Penstemon	Collier		48.85		−25.37		1.258		−4.27	
JRH160729B	Aster	Gotchen		43.28	0.10	−28.94	0.56	3.568		−5.01	
JRH160729N	Lupine	Gotchen		44.01	0.29	−28.11	0.52	4.454	0.601	−0.93	0.18
JRH160731N	Lupine	Eliot		42.57	0.61	−28.00	0.04	1.873		−0.67	
JRH160731A	Succulent	Eliot		42.96		−28.44		1.689		−0.01	
150625Q-GR1A	Grass	Collier		41.74	0.43	−28.46	0.54	2.200	0.430	−7.43	0.35
150625Q-GR1	Grass	Collier		41.26		−28.28		2.857		−7.38	
150625P-GR2	Grass	Collier		36.76		−26.57		*1.158*		bdl	
JRH160806D	Grass	Collier		41.31		−27.99		2.596		−5.22	
JRH160802C	Grass	Diller		40.88		−25.45		1.130		−5.82	
JRH160802B	Grass	Diller		36.11		−29.09		2.354		−4.05	
JRH160729D	Grass	Gotchen		44.29	1.38	−26.03	0.18	2.032	0.313	−4.39	0.70
JRH160731C	Grass	Eliot		43.73		−27.72		1.413		−3.80	
JRH160806C	Grass	Collier		39.66		−28.20		3.023		−5.81	
JRH160729O	Lichen	Gotchen		42.46	0.70	−24.61		1.395		−7.00	
JRH160806G	Moss	Collier		7.81		−26.43	0.01	0.219		*−6.07*	
JRH160729E	Moss	Gotchen		8.86		−26.72	0.07	0.312		−4.97	
JRH160731B	Moss	Eliot		8.45		−28.67	0.08	*0.195*		*−4.58*	
160802C	Moss	Diller		40.99	0.22	−25.38		0.993	0.078	−3.95	
150625P-SPDR	Spider	Collier		47.46		−24.68		11.025		4.96	
150625P-LDY	Ladybug	Collier		46.71		−27.42		11.247		4.55	
150625P-FLY	Fly	Collier		45.52		−25.36		12.757		3.22	
150625P-CRB	Beetle	Collier		46.97		−24.73		10.274		3.09	
150625P-WASP	Wasp	Collier		48.33		−25.68		9.985		1.20	
150625P-BUG	Bug	Collier		46.25		−21.10		11.205		−0.09	
150625P-RBBE	Beetle	Collier		54.57		−24.01		7.703		−0.59	
JRH160729G	Bug	Gotchen		46.26		−26.20		12.067		1.78	
JRH160729J	Beetle	Gotchen		52.22		−21.96		9.748		−2.33	
JRH160729H	Wasp	Gotchen		50.63		−20.41		11.061		0.92	
JRH160729I	Ladybug	Gotchen		61.34		−26.78		5.571		0.58	
JRH160731I	Ladybug	Eliot		62.59	4.22	−28.17	0.07	6.339		1.11	
JRH160731H	Honey Bee	Eliot		*46.22*		−25.54		11.102		−0.60	
JRH160806H	Hoverfly	Collier		47.04		−25.58		11.898		−2.86	
JRH160731J	Hoverfly	Eliot		41.19	3.16	−26.19	0.05	11.870		−1.61	

S.D. = standard deviation, given for all samples with more than one analysis. bdl = below detection limit. Values in italics are near the limits of calibration curves, and should be taken as approximations. Sample IDs with an asterisk indicate values reported in Hamilton and Havig (2017), with a double asterisk indicating value reported in Hamilton and Havig (2018).

an amalgamation of ~10 individuals). The ranges of values for the contextual samples were as follows: soils: $\delta^{13}C = -26.56$ to $-24.75‰$, $\delta^{15}N = 1.14$ to $2.57‰$; grasses: $\delta^{13}C = -29.09$ to $-25.45‰$, $\delta^{15}N = -7.43$ to $-3.80‰$; evergreen tree needles (pine and hemlock): $\delta^{13}C = -28.40$ to $-22.90‰$, $\delta^{15}N = -8.90$ to $1.76‰$; broadleaf plants: $\delta^{13}C = -29.64$ to $-25.37‰$, $\delta^{15}N = -5.65$ to $-4.27‰$; lupines: $\delta^{13}C = -28.11$ to $-28.00‰$, $\delta^{15}N = -0.67$ to $-0.93‰$; succulent: $\delta^{13}C = -28.44‰$, $\delta^{15}N = -0.01‰$; mosses and lichens: $\delta^{13}C = -28.67$ to $-25.38‰$, $\delta^{15}N = -7.00$ to $-3.95‰$; insects: $\delta^{13}C = -28.17$ to $-20.41‰$, $\delta^{15}N = -2.86$ to $4.96‰$, and ice worms: $\delta^{13}C = -25.90‰$, $\delta^{15}N = -1.80‰$ (Table 1).

3.3. Carbon uptake

The potential for light-dependent and dark inorganic carbon assimilation was assessed across sample locations and sample types (Figs. 2–4, Table 2). Rates of light-dependent carbon uptake were greater than rates of dark carbon fixation in the majority of the sites. In sediments from the moraine-dammed terminal lake at the base of Gotchen Glacier, light-independent inorganic assimilation rates were indistinguishable from microcosms exposed to light (Fig. 2). The highest rates of inorganic carbon assimilation were observed in an outwash biofilm on Eliot Glacier (E1) and supraglacial snow algae on Collier Glacier and a side seep at near Collier Glacier outwash (C4). Rates of light-dependent inorganic carbon assimilation at sites E3 (48.69 ± 1.56 μg C uptake/g $C_{biomass}$/h), C1 (51.66 ± 6.57 μg C uptake/g $C_{biomass}$/h), and C4 (50.70 ± 4.95 μg C uptake/g $C_{biomass}$/h) were over an order of magnitude greater than the values observed for microcosms from these sites performed in the dark. The lowest uptake rates in the light that were still higher than coeval incubations in the dark were found at Gotchen Glacier sites G3 (5.97 ± 1.99 μg C uptake/g $C_{biomass}$/h) and G4 (3.99 ± 0.55 μg C uptake/g $C_{biomass}$/h); Eliot Glacier site E5 (2.87 ± 0.68 μg C uptake/g $C_{biomass}$/h); and Collier Glacier site C3 (1.15 ± 0.17 μg C uptake/g $C_{biomass}$/h). One site (G5) returned uptake values that were elevated but with light and dark values that were indistinguishable (2.89 ± 0.68 μg C uptake/g $C_{biomass}$/h vs. 3.73 ± 2.09 μg C uptake/g $C_{biomass}$/h, respectively).

3.4. Geochemical analyses

Water chemistry was analyzed to examine changes with flow and for comparison between sites. Analyses included *in situ* (pH, conductivity, temperature, NH_4(T), NO_2^-, and NO_3^-), dissolved inorganic carbon (DIC), dissolved organic carbon (DOC), cations (Na, K, Ca, and Mg), and trace elements (P, Al, Ti, Mn, Fe, and Si) (Tables 3a and 3b). pH values were between 4.3, measured in the runoff of Collier Glacier, and 8.1 measured in a distal emerging spring near North Sister. Conductivity values ranged from a high of 25.9 μS/cm to a low of 0.97 μS/cm. Temperatures were generally higher in standing water and distal springs (3.3–15.7 °C) than in supraglacial and subglacial water sampling sites (1.1–4.3 °C). Nearly half of the sites where NH_4(T) analyses were conducted (8 of 18) had values below detection limits, while those above detection limits ranged from 0.92 to 10.35 μmol/L. NO_2^- values ranged between 0.06 and 2.58 μmol/L. NO_3^- values fell between 0.16 and 1.94 μmol/L.

The lowest DIC concentration observed was 9.15 μmol/L returned from melted glacial ice from Eliot Glacier. The highest concentration was 331.30 μmol/L recovered from a distal spring near North Sister. DIC field blank concentration values were 3.192–39.36 μmol/L, representing equilibration of the 18.2 MΩ/cm deionized water with the atmosphere during transport from the lab to the field site. DIC $\delta^{13}C$ values ranged from a low of $-22.19‰$ (distal spring) to a high of $-2.91‰$ recovered from the outwash coming out from under the last portion of Collier Glacier ice. DOC concentration values were consistently near or greater than DIC concentrations for nearly all sites and fell between a 24.12 μmol/L at the Eliot Glacier outwash site

Table 2
Carbon uptake assay results.

Gotchen Glacier		Average	S.D.	Eliot Glacier		Average	S.D.	Collier Glacier		Average	S.D.
G1	Light	27.51	0.50	E1	Light	42.95	0.36	C1	Light	51.66	6.57
	Dark	3.40	0.84		Dark	−0.07	0.15		Dark	3.97	1.88
	Photo(Net)	**24.11**			Photo(Net)	**43.03**			Photo(Net)	**47.69**	
G2	Light	29.61	1.76	E2	Light	6.47	3.22	C2	Light	12.45	3.04
	Dark	1.77	0.91		Dark	0.77	0.51		Dark	0.57	0.10
	Photo(Net)	**27.83**			Photo(Net)	**5.71**			Photo(Net)	**11.88**	
G3	Light	5.97	1.99	E3	Light	48.69	1.56	C3	Light	1.15	0.17
	Dark	0.53	0.13		Dark	0.70	0.24		Dark	−0.26	0.14
	Photo(Net)	**5.44**			Photo(Net)	**47.99**			Photo(Net)	**1.41**	
G4	Light	3.99	0.54	E4	Light	16.31	4.29	C4	Light	50.70	4.95
	Dark	1.22	0.58		Dark	3.75	0.68		Dark	4.61	2.51
	Photo(Net)	**2.77**			Photo(Net)	**12.56**			Photo(Net)	**46.09**	
G5	Light	2.89	0.68	E5	Light	2.87	0.68	C5	Light	11.93	0.88
	Dark	3.73	2.09		Dark	0.57	0.09		Dark	1.31	0.19
	Photo(Net)	**−0.83**			Photo(Net)	**2.30**			Photo(Net)	**10.62**	

Bold values indicate calculated Photo(Net) values (Light minus Dark treatment average values).
S.D. = standard deviation. All values given in units of μg C uptake/g $C_{biomass}$/h.

Table 3a
Aqueous geochemistry results, part 1. Location, date and time of collection, pH, conductivity, temperature, total ammonia ($NH_4(T)$), nitrite (NO_2^-), nitrate (NO_3^-), dissolved inorganic carbon (DIC), dissolved inorganic carbon $\delta^{13}C$ values, dissolved organic carbon (DOC), and dissolved organic carbon $\delta^{13}C$ values.

Sample ID	Location	C uptake ID	10 T	UTM	Elevation (m)	Date	Time of collection	pH	Conductivity µS/cm	Temperature (°C)	$NH_4(T)$ µmol/L	NO_2^- µmol/L	NO_3^- µmol/L	DIC µmol/L	$\delta^{13}C_{VPDB}$ ‰	DOC µmol/L	$\delta^{13}C_{VPDB}$ ‰
Gotchen Glacier, Mt. Adams, WA																	
160728A	Gotchen Glacier Lake	G5	0618018	5112972	2170	07/28/16	10:15	5.56	2.81	3.4	1.29	0.26	0.54	20.40	-8.49	nd	nd
160728B	Red Algae Inc Site Snow	G1	0617918	5112950	2183	07/28/16	09:45	4.73	15.71	0.0	bdl	0.56	1.94	23.48	-14.57	126.70	-22.49
160729D	Orange Algae Incubation	G2	0617927	5112924	2178	07/29/16	10:00	nd	nd	nd	nd	nd	nd	nd	nd	nd	nd
160729F	Snow edge sed inc	G3	0617918	5112975	2175	07/29/16	10:25	nd	nd	nd	nd	nd	nd	nd	nd	nd	nd
160729G	Dirty snow inc	G4	0617918	5112975	2175	07/29/16	10:35	nd	nd	nd	nd	nd	nd	nd	nd	nd	nd
Eliot Glacier, Mt. Hood, OR																	
160730A	Orange Algae Snow	E1	0604028	5026596	2128	07/30/16	16:41	5.34	2.56	0.0	nd	nd	nd	9.19	bdl	46.29	bdl
160730B	Glacial Outwash	E5	0604039	5026653	2106	07/30/16	15:25	5.65	3.26	1.2	bdl	0.43	1.13	17.23	-8.94	24.12	bdl
160730C	Tan foamy seds	E4	0604039	5026654	2106	07/30/16	15:50	nd	nd	nd	nd	nd	nd	nd	nd	nd	nd
160730D	Edge Algae Inc	E2	0604027	5026596	2128	07/30/16	16:41	nd	nd	nd	nd	nd	nd	nd	nd	nd	nd
160730E	Dirty Snow		0604027	5026596	2128	07/30/16	16:41	nd	nd	nd	nd	nd	nd	nd	nd	nd	nd
160730F	Glacial Ice		0604043	5026644	2108	07/30/16	16:45	5.66	3.00	0.0	nd	nd	nd	10.46	bdl	96.15	bdl
160730G	Glacial Outwash		0604039	5026653	2106	07/30/16	20:00	5.60	2.89	1.1	bdl	0.20	0.70	18.08	-8.93	28.78	bdl
160731H	Glacial Outwash		0604039	5026653	2106	07/31/16	06:45	5.58	3.27	1.6	bdl	0.28	0.65	16.89	-8.73	36.70	bdl
160731I	White biofilm under seds	E3	0604039	5026652		07/31/16	07:40	nd	nd	nd	nd	nd	nd	nd	nd	nd	nd
160731K	Glacial Outwash		0604039	5026653	2106	07/31/16	10:25	5.57	3.07	1.2	bdl	1.88	1.51	17.54	-8.67	39.20	bdl
160731L	Spring emerging along trail		0604995	5027560	1902	07/31/16	13:18	6.65	37.24	4.0	nd	nd	nd	131.86	-18.57	78.02	bdl
Diller Glacier, Middle Sister, OR and Collier Glacier, North Sister, OR																	
160802A	Diller South Beach (Lake)		0598963	4888222	2276	08/02/16	16:30	6.82	4.14	15.71	bdl	0.88	1.34	22.29	-9.31	54.85	bdl
160802B	Dirty Orange Snow		0598957	4888213	2276	08/02/16	16:46	5.48	4.46	1.5	nd	nd	nd	55.13	-17.54	628.94	-11.39
160802C	Seep below Diller Moraines		0599249	4888430	2201	08/02/16	17:51	7.12	14.41	3.3	nd	nd	nd	86.65	-8.55	72.62	bdl
160806A	Upper Runoff 1		0596888	4891608	2264	08/06/16	06:50	6.88	4.09	1.1	10.35	0.37	0.54	33.95	-7.54	nd	nd
160806B	Collier's Spa (Lake)	C5	0596766	4892848	2119	08/06/16	10:00	6.78	4.88	11.6	bdl	0.86	0.75	35.27	-4.12	31.68	bdl
160806C	Collier Bubbler	C4	0596764	4892631	2135	08/06/16	10:45	*5.5*	24.8	5.8	nd	nd	nd	nd	nd	nd	nd
160806D	Collier Base Outwash		0596679	4892382	2131	08/06/16	11:25	*5.3*	5.14	4.3	6.84	0.95	bdl	34.64	-2.91	49.76	bdl
160806E	Upper Runoff 2		0596888	4891608	2264	08/06/16	12:50	*5.0*	4.80	1.4	7.03	0.37	bdl	32.94	-7.25	34.94	bdl
160806F	Supraglacial runoff		0596903	4891556	2301	08/06/16	13:56	*4.9*	0.97	1.1	bdl	0.23	1.02	16.90	-8.80	51.02	bdl
160806G	Red Snow Inc Site	C1	0596845	4891574	2284	08/06/16	14:35	*4.5*	1.95	0.0	0.92	0.35	1.83	10.64	bdl	83.94	bdl
160806H	Muddy snow inc	C2	0596888	4891575	2267	08/06/16	15:10	nd	nd	nd	nd	nd	nd	nd	nd	nd	nd
160806I	Upper Runoff seds inc	C3	0596888	4891608	2264	08/06/16	15:45	nd	nd	nd	nd	nd	nd	nd	nd	nd	nd
160806J	Upper Runoff 3		0596888	4891608	2264	08/06/16	17:00	*5.0*	3.46	1.2	6.10	2.58	bdl	27.71	-7.94	37.09	bdl
160806K	Glacier Ice		1596854	4891589	2292	08/06/16	17:30	*4.5*	3.80	0.0	4.99	0.06	bdl	9.15	bdl	39.48	bdl
160806L	Upper Runoff 4		0596888	4891608	2264	08/06/16	19:00	*4.3*	4.00	1.1	7.21	0.67	0.16	28.82	-7.42	95.64	bdl
160807M	Garden of Bubbles		0596777	4891587	2289	08/07/16	19:22	*4.7*	1.49	1.1	3.70	0.36	0.38	17.58	-9.91	47.60	bdl
160807N	Upper Runoff 5		0596888	4891608	2264	08/07/16	09:30	*4.7*	5.44	1.3	6.47	0.27	bdl	34.87	-7.02	31.37	bdl
160807P	Spring feeding Spring Lake		0591335	4893670	1602	08/07/16		8.07	25.9	10.2	nd	nd	nd	331.30	-22.19	101.05	bdl
Field Blanks																	
160729H	Field Blank					07/29/16		nd	nd	nd	nd	nd	nd	35.89	bdl	52.27	-28.71
160731J	Field Blank					07/31/16		nd	nd	nd	nd	nd	nd	31.92	bdl	45.57	-25.18
160807O	Field Blank					08/07/16		nd	nd	nd	nd	nd	nd	39.36	bdl	132.73	-23.52

$NH_4(T)$, NO_3^-, and NO_2^- determined via spectrophotometry. Dissolved inorganic carbon (DIC) and dissolved organic carbon (DOC) determined via isotope ratio mass spectrometry.
nd = not determined, bdl = below detection limits. pH in italics denotes determination via pH paper. Values in grey have been reported previously (Rutledge et al., 2018).

and 628.94 µmol/L recovered from the Diller Glacier snow algae site. Field blank DOC concentrations (45.57–132.73 µmol/L) were similar to those measured for most sites, suggesting DOC concentrations may be attributable to background contamination. The Diller Glacier snow algae site was the only sample with a concentration value that fell above field blank values. The $\delta^{13}C$ in DOC from Diller Glacier snow algae was −11.39‰.

Elements measured via ICP-OES include dominant cations (Na, K, Mg, Ca) as well as P and Si. Na concentration ranged from 0.56 to 83.86 µmol/L, with field blank values ranging from below detection limits (bdl) to 25.89 µmol/L. K concentration ranged from 0.41 to 27.19 µmol/L, with field blank values ranging from 0.59 to 7.49 µmol/L. Mg concentration ranged from 0.12 to 20.70 µmol/L, with field blank values falling at or below 0.23 µmol/L. Ca concentration ranged from 0.89 to 54.12 µmol/L, while field blank values fell between 0.21 and 0.68 µmol/L. There was a general trend of lower cation concentration in supraglacial samples, higher cation concentration in subglacial/outwash samples, and the highest cation concentration values in the distal springs. P concentration values were bdl (<0.81 µmol/L) for most sites (including all water samples from Gotchen Glacier, all water samples from Eliot Glacier, and most supraglacial samples from Diller and Collier Glaciers). In Collier Glacier subglacial samples and distal springs at Diller, Collier, and Eliot Glaciers, P concentration values ranged from 0.85 to 2.27 µmol/L. Dissolved Si concentration (reported as SiO_2) for all glaciers sampled exhibited a general trend of supraglacial sites < subglacial/outwash sites < distal springs, with values ranging between 0.29 µmol/L recovered from melted Eliot Glacier ice and 415.39 µmol/L recovered from an emergent spring adjacent to Eliot Glacier. In field blank, Si values at or below 3.46 µmol/L were observed. All water samples below 3.46 µmol/L are considered indistinguishable from the field blank.

Elements measured via ICP-MS include the trace elements Al, Ti, Mn, and Fe. Al concentration values fell between 0.12 and 5.42 µmol/L, consistently at or above the values recovered from field blanks (0.04–0.18 µmol/L). Al concentration values were generally lower for Gotchen and Eliot Glacier sites compared to Collier and Diller Glaciers, where supraglacial sites were lower than subglacial/outwash sites. Ti concentration values ranged from 1.55 to 471.39 nmol/L, with only five samples falling in the range of field blank values (≤3.09 nmol/L). The highest values were returned from subglacial samples at Collier Glacier (≥300.39 nmol/L). Mn concentration values fell between 1.11 nmol/L recovered from Eliot Glacier snow and 117.90 nmol/L recovered from Diller Glacier snow, with most values falling above the field blank range of 0.69 to

Table 3b
Aqueous geochemistry results, part 2. Phosphorous (P), sodium (Na), potassium (K), calcium (Ca), magnesium (Mg), silicon (Si), aluminum (Al), titanium (Ti), manganese (Mn), and iron (Fe).

Sample ID	Location	C uptake ID	P µmol/L	Na µmol/L	K µmol/L	Ca µmol/L	Mg µmol/L	Si µmol/L	Al µmol/L	Ti nmol/L	Mn nmol/L	Fe nmol/L
Gotchen Glacier, Mt. Adams, WA												
160728A	Gotchen Glacier Lake	G5	bdl	8.35	1.02	4.89	0.99	26.71	0.66	13.60	9.81	79.7
160728B	Red Algae Inc Site Snow	G1	bdl	5.60	1.71	2.42	1.13	0.85	0.50	5.70	73.66	1758
160729D	Orange Algae Incubation	G2	nd	nd	nd	nd	nd	nd	nd	nd	nd	nd
160729F	Snow edge sed inc	G3	nd	nd	nd	nd	nd	nd	nd	nd	nd	nd
160729G	Dirty snow inc	G4	nd	nd	nd	nd	nd	nd	nd	nd	nd	nd
Eliot Glacier, Mt. Hood, OR												
160730A	Orange Algae Snow	E1	bdl	0.56	bdl	0.89	0.12	0.58	0.28	3.61	1.11	100
160730B	Glacial Outwash	E5	bdl	1.86	0.4	7.42	2.44	4.75	0.14	2.07	60.36	36.6
160730C	Tan foamy seds	E4	nd	nd	nd	nd	nd	nd	nd	nd	nd	nd
160730D	Edge Algae Inc	E2	nd	nd	nd	nd	nd	nd	nd	nd	nd	nd
160730E	Dirty Snow		nd	nd	nd	nd	nd	nd	nd	nd	nd	nd
160730F	Glacial Ice		bdl	8.33	2.9	1.19	0.28	0.29	0.17	4.30	9.59	38.1
160730G	Glacial Outwash		bdl	2.55	bdl	7.71	2.48	6.10	0.56	4.37	57.34	82.1
160731H	Glacial Outwash		bdl	2.33	bdl	8.51	2.89	6.53	0.15	1.80	61.38	35.2
160731I	White biofilm under seds	E3	nd	nd	nd	nd	nd	nd	nd	nd	nd	nd
160731K	Glacial Outwash		bdl	2.20	bdl	7.92	2.63	8.19	0.16	3.32	57.72	41.9
160731L	Spring emerging along trail		1.43	83.86	27.2	54.12	10.34	415.39	0.24	1.55	3.13	22.3
Diller Glacier, Middle Sister, OR and Collier Glacier, North Sister, OR												
160802A	Diller South Beach (Lake)		bdl	8.23	0.80	4.17	1.58	26.16	1.09	31.66	23.85	218
160802B	Dirty Orange Snow		bdl	4.66	1.89	1.18	0.61	1.79	0.30	3.30	117.90	93.1
160802C	Seep below Diller Moraines		1.77	69.86	8.44	26.65	14.16	148.88	1.31	39.35	5.61	280
160806A	Upper Runoff 1		1.60	25.99	2.19	9.35	6.97	48.24	4.20	381.58	49.66	2493
160806B	Collier's Spa (Lake)	C5	1.07	26.84	2.75	8.58	5.73	55.82	3.87	220.76	36.28	1603
160806C	Collier Bubbler	C4	nd	nd	nd	nd	nd	nd	nd	nd	nd	nd
160806D	Collier Base Outwash		2.08	27.19	2.38	9.88	7.86	53.50	5.42	471.39	62.83	3151
160806E	Upper Runoff 2		1.94	24.72	2.48	8.94	6.85	48.82	4.97	430.66	56.65	2818
160806F	Supraglacial runoff		bdl	0.65	bdl	0.89	0.74	1.06	0.12	2.53	37.88	33.3
160806G	Red Snow Inc Site	C1	0.93	12.24	1.62	1.36	0.28	0.76	0.26	6.77	4.55	91.6
160806H	Muddy snow inc	C2	nd	nd	nd	nd	nd	nd	nd	nd	nd	nd
160806I	Upper Runoff seds inc	C3	nd	nd	nd	nd	nd	nd	nd	nd	nd	nd
160806J	Upper Runoff 3		1.47	16.82	1.61	6.88	5.25	30.81	3.79	313.49	44.56	2079
160806K	Glacier Ice		bdl	8.92	0.99	1.41	0.75	4.04	1.14	54.01	11.72	384
160806L	Upper Runoff 4		1.30	18.80	1.69	7.38	5.67	35.93	3.67	300.75	42.10	2047
160807M	Garden of Bubbles		bdl	2.22	bdl	1.11	0.56	1.56	0.21	6.02	7.83	52.8
160807N	Upper Runoff 5		2.27	27.87	2.19	9.89	7.39	51.09	4.09	347.74	46.03	2369
160807P	Spring feeding Spring Lake		0.85	50.94	8.93	41.04	20.70	207.44	0.40	1.80	50.00	53.1
Field Blanks												
160729H	Field Blank		bdl	bdl	bdl	0.21	bdl	3.46	0.04	bdl	0.84	318
160731J	Field Blank		bdl	1.43	0.59	0.23	0.04	0.60	0.06	2.34	0.69	22.1
160807O	Field Blank		1.03	25.89	7.49	0.68	0.23	bdl	0.18	3.09	5.55	70.7

P, Na, K, Ca, Mg, and Si determined via inductively coupled plasma optical emission spectroscopy. Al, Ti, Mn, and Fe determined via inductively coupled plasma mass spectrometry. nd = not determined, bdl = below detectin limits. Values in grey have been reported previously (Rutledge et al., 2018).

5.50 nmol/L. Fe concentration values field blank values ranged from 22.1 to 318 nmol/L, and most samples fell within this range except for all subglacial/outwash samples from Collier Glacier (1603–3151 nmol/L) and the snow sample from Gotchen Glacier (1758 nmol/L). For all trace elements, the highest concentrations were recovered from subglacial/outwash samples from Collier Glacier.

4. DISCUSSION

Subglacial microbial communities may drive chemical weathering through proton generation in glaciers hosted in mineral-containing rocks (e.g., irons sulfides) (Sharp et al., 1999; Foght et al., 2004; Wynn et al., 2006; Hamilton et al., 2013; Mitchell et al., 2013; Boyd et al., 2014; Telling et al., 2015). Primary productivity on supraglacial surfaces is a key process in glacial ecosystems and weathering and previous studies have observed connectivity between supra- and subglacial microbial communities (Hodson et al., 2005; Wynn et al., 2006; Boyd et al., 2011, 2014; Hamilton et al., 2013; Hotaling et al., 2017).

Recent work has suggested a high release of dissolved silica and cations from mineral weathering in volcanic rock-hosted glacial systems, likely driven by generation of protons from formation and deprotonation of carbonic acid (i.e., $CO_2 + H_2O \Rightarrow H^+ + HCO_3^-$), occurs in the subglacial environment of volcanics-hosted glacial systems (Rutledge et al., 2018). However, a source for CO_2 beyond atmospheric input was not explored.

In the Pacific Northwest, genes and transcripts of snow algae (predominantly Chlorophyceae (primarily Chlamydomonas) and to a lesser extent Trebouxiophyceae (primarily Prasiolales)) have been recovered from supraglacial snow (Hamilton and Havig, 2017, 2018) where inorganic

carbon uptake microcosms indicate photosynthesis is the dominant primary production process in these systems. Rates of light-dependent inorganic carbon assimilation for these snow algae communities (5.5–51.1 μg C/g $C_{biomass}$/h) are similar to values reported for other sites (Hamilton and Havig, 2017). These studies report on snow algae that bloom on supraglacial snow (e.g., pigment-colored snow/ice observable with the naked eye) while few studies have reported on microbial communities and primary productivity in other supraglacial and periglacial environments in volcanic-hosted terrains such as PNW stratovolcanoes. Furthermore, the source of other elements, especially fixed nitrogen, and the connection of supraglacial productivity to subglacial processes for these systems remains poorly constrained.

From this comprehensive data set we show that microbial community compositions are similar across all sampling sites, that snow algae are the predominant carbon fixation agents across all supraglacial and periglacial environments sampled, that carbon uptake rates vary dramatically across environments, that snow algae have nitrogen requirements met from deposition of fixed nitrogen from anthropogenic sources, and that breakdown of supraglacial-sourced organic carbon contributes to weathering and breakdown of silicate rocks in subglacial environments.

4.1. Characterizing supraglacial communities across a range of environments

4.1.1. What microbial communities inhabit PNW glacial ecosystems?

In this study, we targeted supraglacial snow algae samples as well as proximal sediment samples to begin to constrain the role of these distinct microbiomes in biogeochemical cycling in glacial ecosystems (Figs. 2–4). Despite a sampling strategy to target different niche space

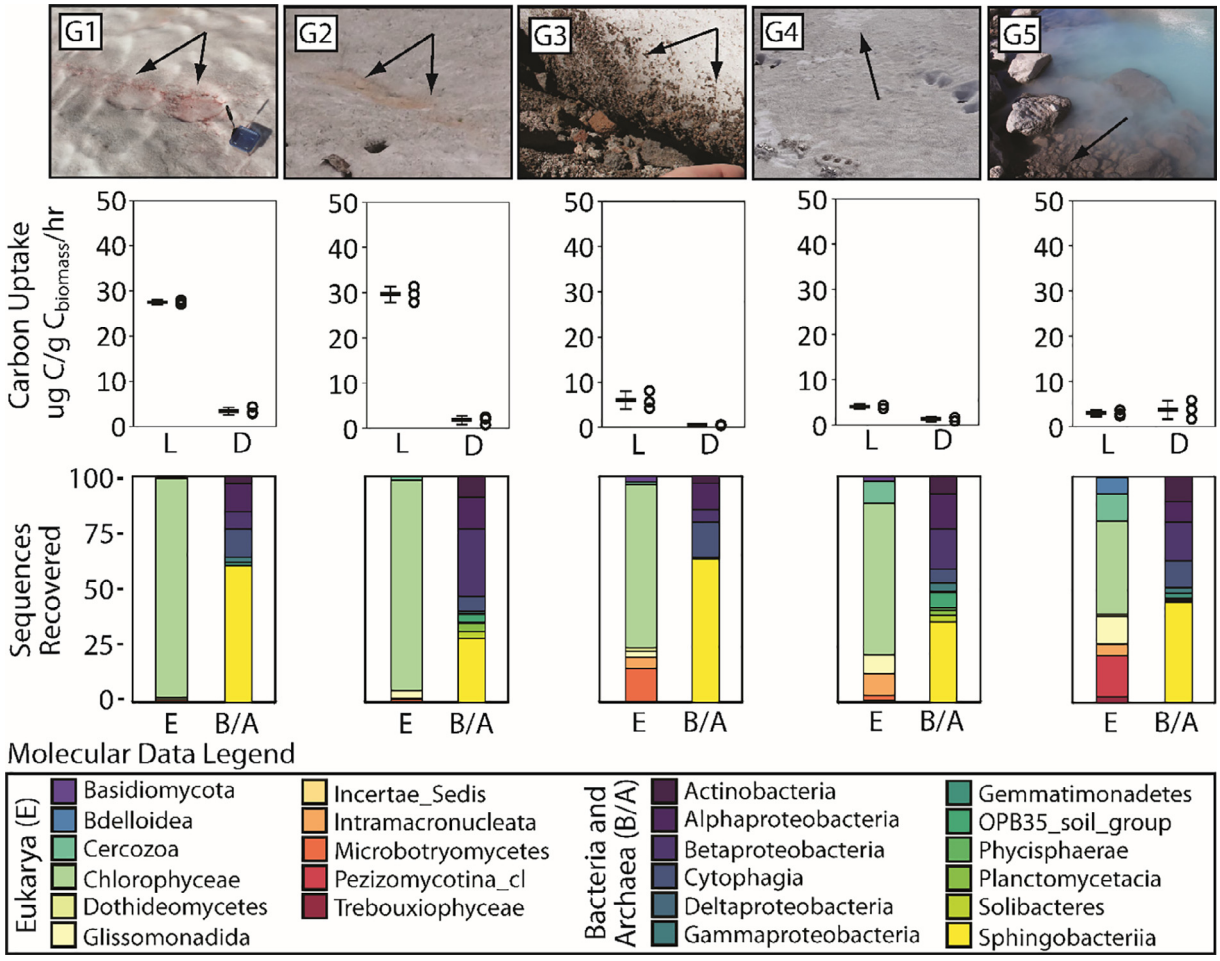

Fig. 2. Locations and images of sample sites (top), carbon uptake incubation rates (middle), and molecular analyses results (bottom) for Gotchen Glacier, Mt. Adams, WA. Top left to right: G1 = red supraglacial snow algae, G2 = orange supraglacial snow algae, G3 = snow edge sediments, G4 = dirty snow, G5 = glacial lake sediments. Arrows indicate areas of sample collection. Carbon uptake results (middle) for light (L) and dark (D) treatments show the mean value (filled black bar) with error bars indicating standard deviations next to individual replicate results (open circles). Molecular rRNA sequencing results (bottom) for 18S (Eukarya, or E) and 16S (Bacteria and Archaea, or B/A) shown at the Class level. Predominant snow algae OTUs fell into the class Chlorophyceae (primarily Chlamydomonas) and Trebouxiophyceae (primarily Prasiolales). (For interpretation of the references to colour in this figure legend, the reader is referred to the web version of this article.)

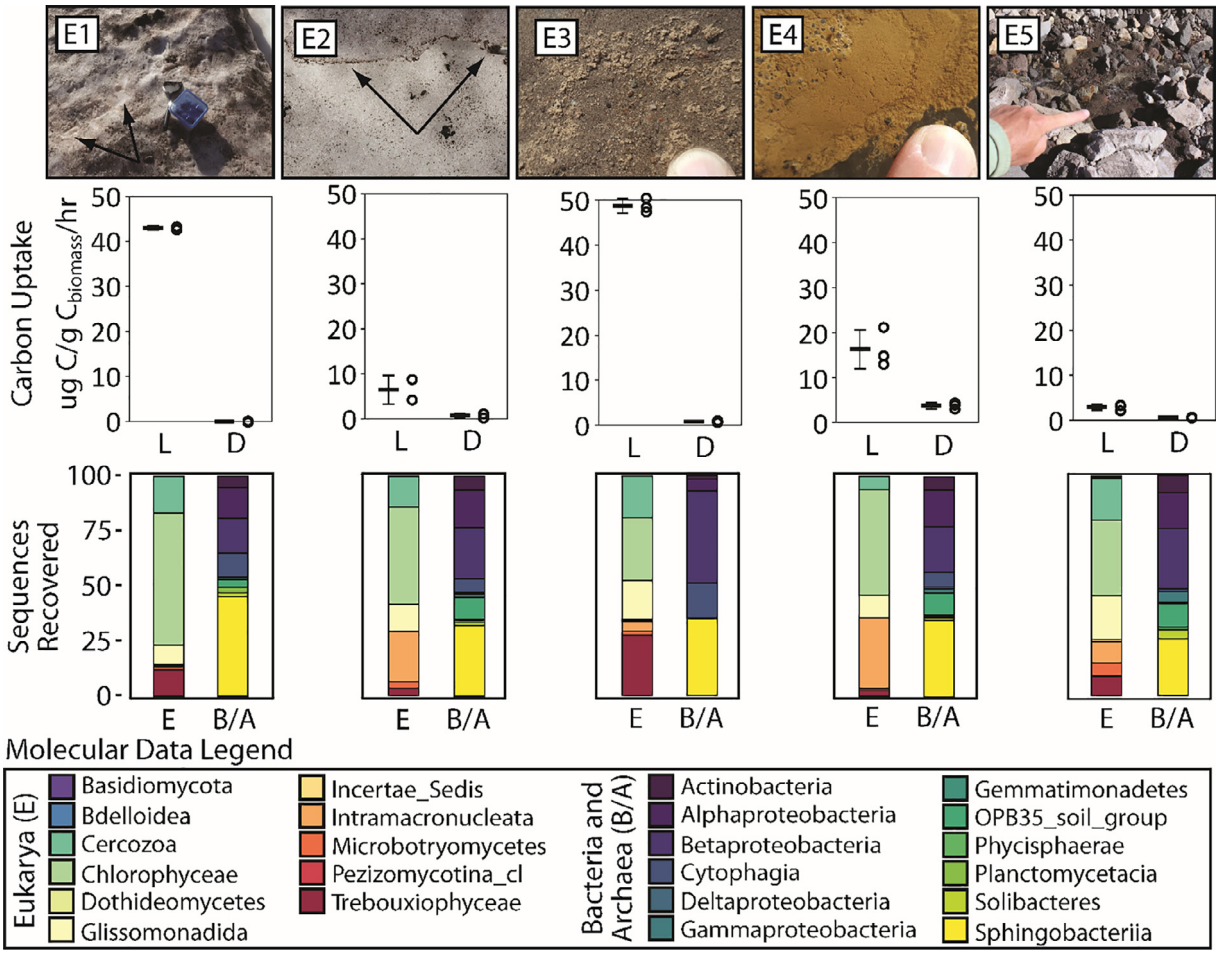

Fig. 3. Locations and images of sample sites (top), carbon uptake incubation rates (middle), and molecular analyses results (bottom) for Eliot Glacier, Mt. Hood, OR. Top left to top right: E1 = red supraglacial snow algae, E2 = snow edge sediments, E3 = outwash biofilm, E4 = foamy tan outwash sediments, E5 = glacial outwash sediments. Arrows indicate areas of sample collection. Carbon uptake results (middle) for light (L) and dark (D) treatments show the mean value (filled black bar) with error bars indicating standard deviations next to individual replicate results (open circles). Molecular rRNA sequencing results (bottom) for 18S (Eukarya, or E) and 16S (Bacteria and Archaea, or B/A) shown at the Class level. Predominant snow algae OTUs fell into the class Chlorophyceae (primarily Chlamydomonas) and Trebouxiophyceae (primarily Prasiolales). (For interpretation of the references to colour in this figure legend, the reader is referred to the web version of this article.)

on and near the glacial surface, the microbial communities recovered in the present study were comprised predominantly of eukaryotic photoautotrophic algae and heterotrophic bacteria. In the case of supraglacial snow samples, these results are consistent with previous studies (e.g., Lutz et al., 2015; Hamilton and Havig, 2017; Lutz et al., 2017a; Hamilton and Havig, 2018), indicating supraglacial microbiomes are comprised of phototrophic carbon fixers and heterotrophs that likely feed on the autochthonous products from the phototrophs as well as allochthonous organic material delivered via aeolian deposition.

4.1.1.1. Primary producers. Snow algae, typically unicellular green algae (Chlorophyceae), are observed seasonally on snowpack worldwide. Primary productivity on snow surfaces is attributed to snow algae populations which are often red due to carotenoids that serve as a protective shield against intense UV radiation and to dissipate excess energy. OTUs affiliated with Chlorophyceae were the most abundant recovered across both supraglacial snow and periglacial samples (Figs. 2–4). OTUs affiliated with *Chlamydomonas* and *Chloromonas* were the most abundant Chlorophyceae OTUs we recovered (SOM Fig. 8). The three most abundant OTUs were affiliated with *Chloromonas* and were abundant across all sites, particularly in the snow algae samples. Two OTUs affiliated with *Chlamydomonas* were also abundant across most sample sites (SOM Fig. 8) but less abundant in sediment or sediment-rich samples. *Chlamydomonas* are typically affiliated with red-colored snow (Hoham and Duval, 2001) and are considered a cosmopolitan cryophilic species of algae (Lutz et al., 2017a; Segawa et al., 2018). *Chloromonas* are also commonly observed on snowfields, particularly glacier snow (Lutz et al., 2016; Hamilton and Havig, 2017; 2018). We also recovered smaller numbers of OTUs affiliated with *Hafniomonas*, *Chlorogonium, Chlamydopodium*,

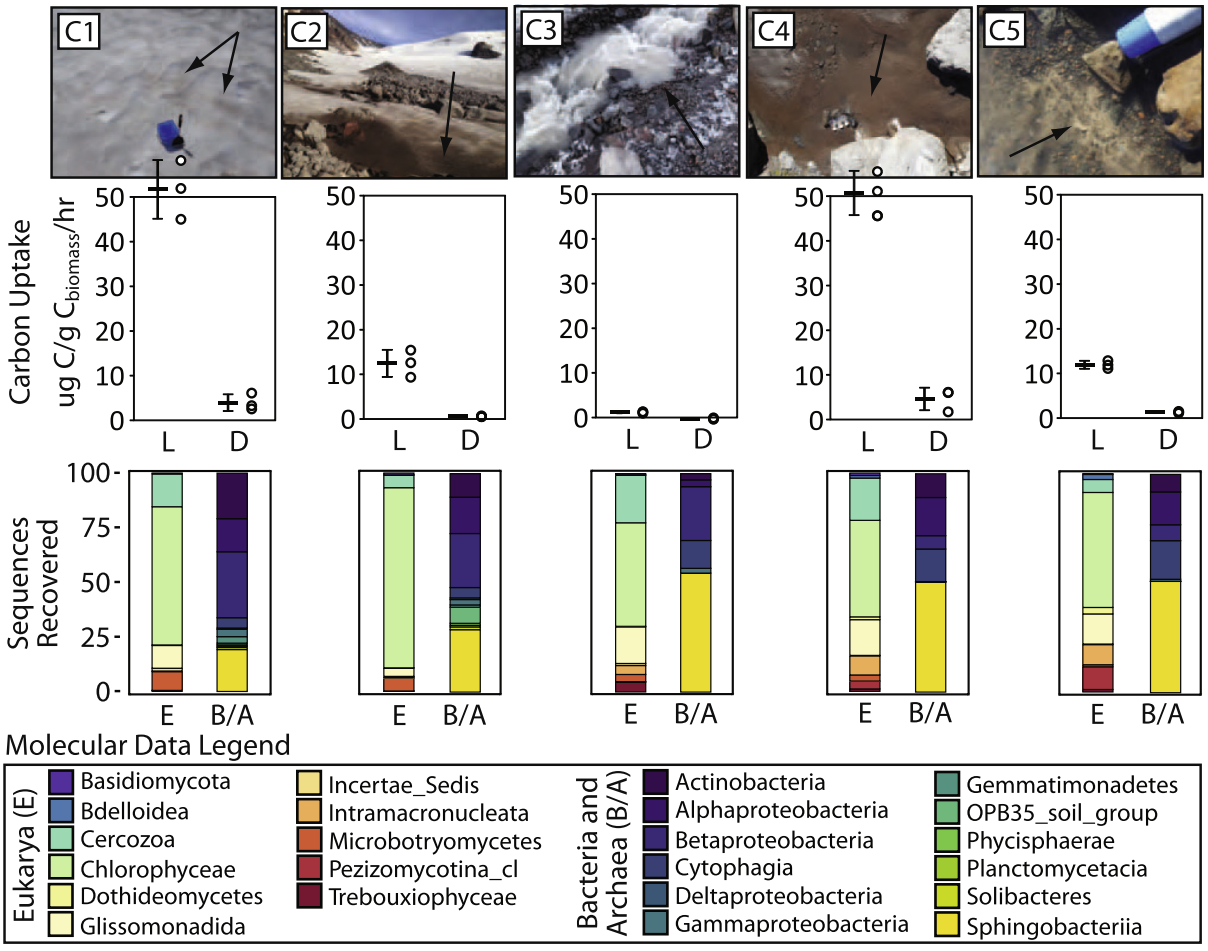

Fig. 4. Locations and images of sample sites (top), carbon uptake incubation rates (middle), and molecular analyses results (bottom) for Collier Glacier, North Sister, OR. Top left to top right: C1 = red supraglacial snow algae, C2 = muddy snow, C3 = outwash sediments, C4 = side seep sediments, C5 = glacial lake sediments with biofilm. Arrows indicate areas of sample collection. Carbon uptake results (middle) for light (L) and dark (D) treatments show the mean value (filled black bar) with error bars indicating standard deviations next to individual replicate results (open circles). Molecular rRNA sequencing results (bottom) for 18S (Eukarya, or E) and 16S (Bacteria and Archaea, or B/A) shown at the Class level. Predominant snow algae OTUs fell into the class Chlorophyceae (primarily Chlamydomonas) and Trebouxiophyceae (primarily Prasiolales). (For interpretation of the references to colour in this figure legend, the reader is referred to the web version of this article.)

Chlainomonas, and *Rhysamphichloris* (SOM Fig. 8). *Chlainomonas* spp. also synthesize red pigments and have been observed in waterlogged snow over ice (Remias et al., 2016). Sequences affiliated with *Chlamydopodium* have been recovered from cold-soil environments (Schmidt et al., 2010), and consistent with this observation, OTUs affiliated with this genus were more abundant in periglacial sediment or sediment-rich samples (SOM Fig. 8). In addition to the abundant Chlorophyceae OTUs, we also recovered OTUs with the green algae Prasiolales, particularly OTUs affiliated with the genus *Stichococcus*. *Stichococcus* are small and resistant to environmental stress, facilitating long-distance dispersal and have been observed in soil from the Arctic and Antarctic (Hodač et al., 2016). In our samples, *Stichococcus* OTUs were particularly abundant in outwash biofilm and sediment samples from Eliot Glacier (Fig. 3).

The 16S rRNA OTUs we recovered were typical of snow and glacial environments— Sphingobacteriia, Betaproteobacteriales and Alphaproteobacteria, Cytophagia, and Actinobacteria. At a higher taxonomic level, these OTUs were affiliated with heterotrophic species including *Solitalea*, *Ferruginibacter*, *Hymenobacter*, and *Polaromonas.* We also recovered sequences affiliated with potential bacterial phototrophs including members of the Cyanobacteria (e.g. *Pseudanabaena* and *Leptolyngbya*) and sequences assigned to the genus *Rhodobacter* in the Alphaproteobacteria. Sequences affiliated with Cyanobacteria were abundant in sediments from Eliot Glacier (E3; SOM Fig. 5); however these OTUs were most closely related to the non-phototrophic Cyanobacteria *Melainabacteria*. *Rhodobacter* are a metabolically diverse genus including members who are phototrophic, lithotrophic, aerobic or anaerobic hindering interoperation of the metabolic potential of these organisms *in situ*. Collectively, OTUs attributed to potential bacterial phototrophs accounted for less than 2% of the total sequences recovered. While we cannot rule out chemoautotrophy or anoxygenic photosynthesis contributing to primary productivity, our data indicate green algae

are responsible for the majority of light-dependent primary productivity in our samples. Consistent with other studies (Tynen, 1970; Hodson et al., 2008; Anesio and Laybourn-Parry, 2012), we also observe sequences affiliated with heterotrophic eukaryotes including protozoa and fungi.

In addition to heterotrophy, a number of the 16S rRNA OTUs recovered could also play a role in nitrogen cycling. For instance, members of the Sphingobacteriia have been implicated in denitrification in cold environments including boreal lakes (Peura et al., 2015) and cryoconites (Segawa et al., 2014). We recovered OTUs affiliated with *Nitrosomonadales* within the Betaproteobacteriales and *Nitrospirales* within the Nitrospirae which have been implicated in nitrification in cryconites (Segawa et al., 2014). We also recovered 16S rRNA OTUs affiliated with *Planctomycetales* which might function as ammonia oxidizers. These data are consistent with potential nitrogen cycling in glacial ecosystems as implicated in other studies (Boyd et al., 2011; Hamilton et al., 2013) and align with values for NH_4(T), NO_2^-, and NO_3^- recovered from supraglacial samples (Table 1 and Fig. 6).

4.2. What factors effect the distribution of microbial communities in PNW glacial ecosystems?

On snow and ice surfaces, microbiota are limited by liquid water and only thrive in the melt season. Other factors that constrain the distribution of snow algae on snowpack remain ambiguous. Some studies indicate no correlation between snow algae abundance and snow nutrient content (Lutz et al., 2016) or no stimulation of snow algae abundance with added nutrients (Hamilton and Havig, 2017). In contrast, others have observed increased snow algae abundance in the presence of added nutrients or coincident with allochthonous bird deposition (Fujii et al., 2010; Musilova et al., 2016; Dial et al., 2018). Here, we examined snow algae microbiomes and surrounding sediments along with a suite of geochemical parameters in snowmelt and glacial outwash and evaluated patterns between OTU abundance, community diversity, and physicochemical parameters using a Spearman correlation-based heat map of the most abundant OTUs (top 50) and environmental variables (SOM Fig. 5). We observed a negative correlation between some of the green algae OTUs and $\delta^{13}C$, nitrite, potassium and nitrate (SOM Fig. 9). A negative correlation was also observed between $\delta^{13}C$ and OTUs assigned to Cercozoa including *Glissomonadida* and. We observed a few strong positive correlations between 18S rRNA OTUs and physicochemical parameters. These included OTUs affiliated with green algae and an OTU affiliated with *Fistulifera* which were positively correlated to total N and total C. These data may indicate higher C and N selects for specific green algae populations. A similar analysis with the top 50 16S rRNA OTUs indicated a negative correlation between nearly all the top 50 OTUs and total N and C (SOM Fig. 10). No strong positive correlations were observed except for an OTU affiliated with *Rickettsia* which was positively correlated with most physicochemical parameters.

Collectively, recovering correlations between physicochemical parameters and snow algae and microbiota are likely complicated by the lack of detectable geochemical parameters in many of our samples. We do observe small differences in composition of snow algae such as the recovery of *Chlamydopodium* and *Stichococcus* from sediment and sediment-rich samples (SOM Fig. 8) suggesting these niches select for different populations of green algae but the contribution of these populations to biogeochemical cycling in glacial and periglacial ecosystems remains unconstrained. One parameter that was not quantified in this study was the presence of liquid water, which constrains the distribution and life span of snow algae — blooms form in the melt season when liquid water is available. This is likely a key factor in snow algae community composition, in addition to nutrient availability as well as sampling time — i.e., peak melt.

4.3. What do microbial biomass C and N isotope values tell us?

Carbon and nitrogen isotopic values were determined for snow algae communities as well as a suite of contextual biological and soil samples from on or near glacier surfaces (Table 1). Plotting $\delta^{15}N$ values versus $\delta^{13}C$ values helps to differentiate patterns of carbon and nitrogen uptake for the sample populations analyzed (Fig. 5). All but one of the multi-cellular plant samples fell between $\delta^{13}C$ values of −25 and −30‰, a typical range for C3 plants, with the average $\delta^{13}C$ value for all plant and lichen samples being −27.15‰ (Table 1 and Fig. 5). Lupine, succulent, and two evergreen needle samples plotted within the field of $\delta^{15}N$ values expected for nitrogen fixed from atmospheric N_2 (with $\delta^{15}N$ value of 0‰) via biological N_2-fixation, resulting in $\delta^{15}N$ values of ~2 to −2‰ (Fig. 5). Forest soils collected from near the glaciers returned $\delta^{13}C$ and $\delta^{15}N$ values that would be expected from broken down biomass of plants that has preferentially liberated ^{12}C and ^{14}N, making their values more positive. Most plants, including all of the moss and lichen samples, returned $\delta^{15}N$ values that were more negative (−2.90 to −8.91‰, average of −5.52‰), suggesting a fixed nitrogen source with a negative $\delta^{15}N$ value (Fig. 5). Given the predominant wind direction from the west, the most likely fixed nitrogen source is assumed to be the ubiquitous animal waste lagoons (especially dairy farms) found in the Portland/Vancouver metropolitan area as well as along the Oregon/Washington coast. From dairy lagoons, isotopically light ammonia was preferentially lost through volatilization to the atmosphere, resulting in NH_3 $\delta^{15}N$ values of −15 to −31‰ over 14 days in one study (Hristov et al., 2009), and observed fractionation factors between aqueous and vapor NH_3 $\delta^{15}N$ values of −5.2 to −10.2‰ (Deng et al., 2018) which are consistent with feed lot-associated NH_3 release $\delta^{15}N$ values of −15 to −9 ‰ (Macko and Ostrom, 1994). A study of NH_4^+ and NO_3^- delivered from rain in Germany showed NH_4^+ concentration was consistently higher than NO_3^-, and NH_4^+ $\delta^{15}N$ values ranged seasonally from −13.7 to −8.8‰ while NO_3^- $\delta^{15}N$ values ranged from −6.4 to +0.8‰ (Freyer, 1978).

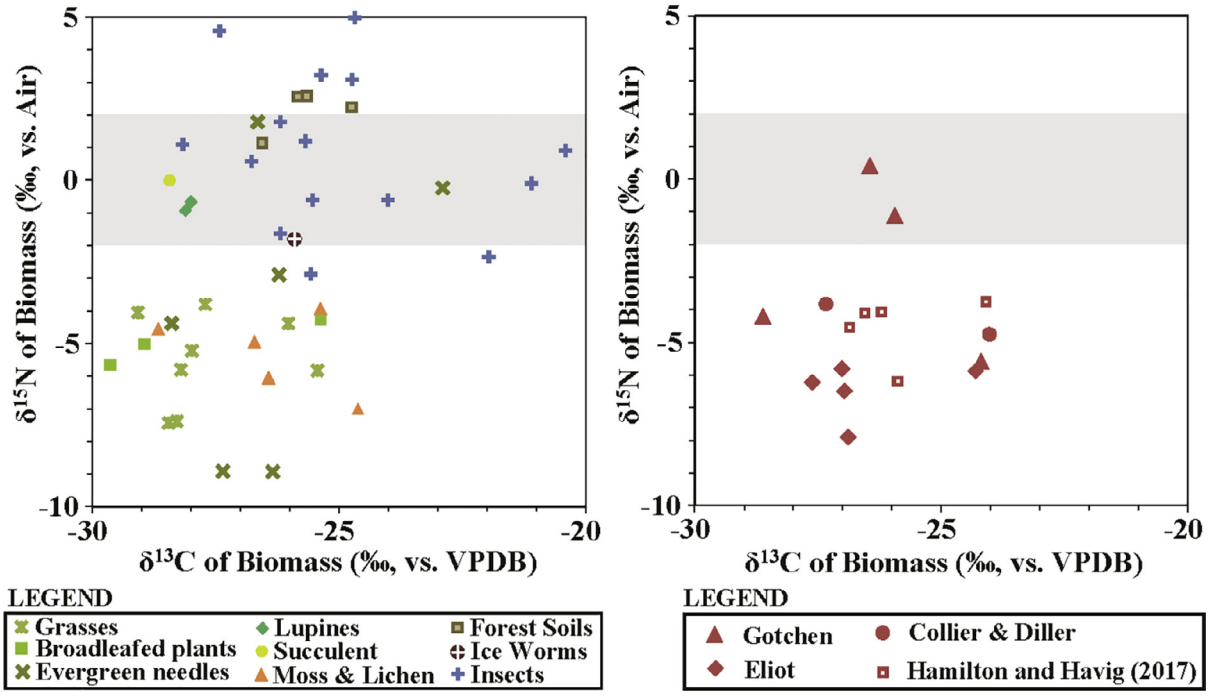

Fig. 5. Carbon and nitrogen stable isotope results for contextual samples (left) and snow algae biomass (right) at Gotchen, Eliot, Palmer, Collier, and Diller Glaciers. Grey shaded area indicates $\delta^{15}N$ values expected for biomass derived from nitrogen fixing organisms.

Another potential source of fixed N is from the ocean, with marine-associated NH_4^+ $\delta^{15}N$ values ranging between −8 and −5‰ (Jickells et al., 2003). Isotopically light fixed N is then delivered to glacial surfaces via precipitation (snow and/or rain) and incorporated into local glacial and periglacial ecosystems, similar to what has been documented in glacial lakes in western North America (Wolfe et al., 2003) as well as for remote watersheds across the Northern Hemisphere (Holtgrieve et al., 2011). Insects found on glacier surfaces ranged in $\delta^{13}C$ values from −28.17 to −20.41‰ and in $\delta^{15}N$ values from −2.86 to 4.96‰, indicating a wide array of C and N sources and trophic levels (Table 1, Fig. 5). Remains of all of these were found scattered across the snow and glacial surfaces, suggesting heterotrophic breakdown of this allochthonous organic material cold provide potential C and N sources for snow algae communities.

Snow algae microbial community samples with C and N values high enough for isotopic determination (including those from Hamilton and Havig, 2017) returned $\delta^{13}C$ values of −28.61 to −24.02‰ with an average of −26.22‰ and $\delta^{15}N$ values of −7.90 to 0.41‰ with an average of −4.63‰ (Table 1 and Fig. 5). While care was taken to remove all visible pieces of organic material from snow algae samples using a dissecting microscope following drying of samples (e.g., insect parts and plant material), allochthonous soil particles and microscopic pieces of organic material are assumed to be incorporated into the bulk snow algae samples. Assuming nearly equal proportions of plant vs. insect material removed from supraglacial snow algae samples, the snow algae microbial community biomass derived from allochthonous organic material would fall between the fields plotted by plant material, forest soils, and insects in the $\delta^{13}C$ versus $\delta^{15}N$ plot (Fig. 5). While two snow algae samples fall in the range expected for incorporation of bulk allochthonous organic material (G3 and G4), most are similar to plants with a predominantly atmospheric fixed N source (Fig. 5). We suspect that samples G3 and G4 have relatively positive $\delta^{15}N$ values (−1.1 and 0.4‰) that can be attributed to significant input of allochthonous organic material delivering fixed N with values similar to those of the meadow soils ($\delta^{15}N = 1.1$–2.6‰), resulting in values falling between the other snow algae samples ($\delta^{15}N = -7.9$ to −3.8‰) and meadow soil values.

4.3.1. Dynamic element cycling in supraglacial microbial communities

Supraglacial and subglacial/outwash samples indicate microbial cycling of fixed nitrogen, with detectable amounts of NH_4(T), NO_2^-, and NO_3^- (Tables 3a and 3b), which is consistent with the recovery of sequences affiliated with potential nitrogen-cycling bacteria (Figs. 2–4) and indicates dynamic cycling of elements by the supraglacial microbial communities. Intense cycling of biologically important elements such as P within supraglacial microbial communities is also supported by the data: (1) dissolved P concentrations are below background levels and/or detection limits for most supraglacial samples; (2) and the highest dissolved P concentrations were recovered from subglacial sources samples (Tables 3a and 3b). One potential source of P delivery to supraglacial surfaces is via aeolian deposition. Local ash and comminuted rock could account for an autochthonous source, but recent work had also shown dust sourced from Asian sources can account for 18–45% of total dust deposition in Sierra Nevada montane forest ecosystems (Aciego et al., 2017). Our interpretation is that most of the autochthonous biomass in the samples collected from supragla-

cial and near-glacial surfaces is derived from primary production by snow algae which generates a $\delta^{13}C$ versus $\delta^{15}N$ signal similar to plants growing on or near the glacial surfaces and are dependent on the same CO_2 and fixed N sources as the snow algae. The heterotrophic members of supraglacial and subglacial/outwash microbial communities rely on snow algae primary productivity for fixed organic carbon, and release NH_3 and P during the breakdown of this organic material (Tables 3a and 3b). This assumption is supported by 18S rRNA sequences recovered from snow algae community sample sites (Figs. 2–4). This interpretation is straightforward for the fixed N source for snow algae communities (precipitation containing NH_3 sourced from animal waste lagoons) but the source of CO_2 is more complicated.

4.3.2. CO_2 source for snow algae

Plants have an extensive biomass-atmosphere interface that allows for direct uptake of atmospheric CO_2, however snow algae are found either in snow with meltwater, or in subaqueous environments. In environments where glaciers are hosted in carbonate rocks, the dependence upon atmospheric CO_2 as an inorganic carbon source is lessened due to the ubiquitous presence of comminuted carbonate rock, which upon dissolution produces HCO_3^- which is available for uptake by phototrophs. In volcanic rock-hosted glacial settings where all the majority of bedrock is silicate minerals, snow algae are dependent upon diffusion of CO_2 from the atmosphere through the snow/water/air interface or upon local heterotrophic breakdown of organic carbon and conversion into CO_2 and may be DIC limited (Hamilton and Havig, 2017, 2018).

All supraglacial and peri-glacial water samples collected had DIC concentrations that were near or below the DIC concentrations measured in 18.2 MΩ/cm deionized water after they were allowed to equilibrate with atmospheric air (Tables 3a and 3b). DIC $\delta^{13}C$ values for most supraglacial and subglacial/outwash samples were more positive than the −9.18 ‰ predicted for equilibrium with atmospheric CO_2 with a $\delta^{13}C$ value of 8‰ and a temperature of 0 °C (Mook et al., 1974), suggesting removal of ^{12}C through uptake by snow algae during photosynthesis. Melted snow samples had DIC $\delta^{13}C$ values of −14.57 and −17.54‰, suggesting the interstitial DIC is sourced from both an atmospheric (−9.18‰) source and heterotrophic breakdown of either allochthonous organic matter (~−26 ‰) and/or autochthonous snow algae biomass (~−26‰), which in these systems are indistinguishable. Only a single DOC sample (snow algae sample from Diller Glacier) had a concentration greater than background, and returned a DOC $\delta^{13}C$ value of −11.39‰, indicating the DOC was a refractory component enriched in ^{13}C and suggesting intense cycling of the DOC pool by the endemic snow algae community (Tables 3a and 3b). DOC concentrations at or below background levels supports breakdown and cycling of DOC in the glacial system. Another source of CO_2 that cannot be ruled out is from the local volcanic vents. Fumaroles and vents were sampled for volcanic gasses including CO_2 at Mt. Shasta (CA), Mt. Hood (OR), and Mt. Rainier and Mt. Baker (WA) within the Cascade Range, returning $\delta^{13}C$ values of −13.5 to −5.9‰ (Symonds et al., 2003). Specifically, samples from Mt. Hood fumaroles near the summit ranged from −9.8 to −8.3 ‰ (Symonds et al., 2003), which are indistinguishable from the values returned from samples collected from Eliot Glacier as part of this study (−8.94 to −8.67‰).

4.3.3. Supraglacial trophic levels

Our contextual isotope data indicate multiple trophic level interactions in supraglacial ecosystems. Ice worms (*Mesenchytraeus solifugus*) are a species of oligochaetes adapted to live solely in snow and ice with a range of low-elevation, temperate glaciers from south-central Alaska to central Oregon (Hartzell et al., 2005; Dial et al., 2016). Ice worms tolerate a narrow range of temperatures (−6.8 to 5 °C; Edwards, 1985), and it has been suggested that ice worms feed primarily on snow algae, coming out at night to feed and then retreating into the glacier for protection from high temperatures during the day (Goodman, 1971). Our results from a group of ice worms collected from Collier Glacier ($\delta^{13}C = -25.90‰$, $\delta^{15}N = -1.80‰$) indicate that their diet likely consists of a mixture of autochthonous and allochthonous organic material found on snow and glacial surfaces.

4.4. Connecting subglacial geochemical processes to supraglacial inputs

Carbonic acid weathering is a primary driver of silicate weathering at Collier and Diller Glaciers, releasing dissolved silica as well as major and trace elements in the process (Rutledge et al., 2018). Carbon uptake as well as C and N concentration and isotope results in this study suggest supraglacial snow algae microbial communities may provide a source of organic carbon to the subsurface, feeding subglacial heterotrophs which in turn can generate CO_2 which converts to H_2CO_3 in solution and can drive silicate mineral weathering. To test this, aqueous geochemistry was assessed through the glacial system (Figs. 6 and 7). Sampling sites were divided by glacial location: supraglacial (water strictly from the surface of the glacier), glacial outwash (with subglacial and supraglacial water inputs), final outwash (draining from the base of the toe of the glacier), glacial lake (impounded by the end moraine at or near the toe of the glacier), and distal spring (springs emerging away from the glacier after flowing through the subsurface).

The highest NH_4(T) and dissolved P concentrations were recovered from glacial outwash and final outflow sites at Collier Glacier (Fig. 6). Breakdown of organic matter delivered from the supraglacial environment is the most likely source for these constituents. While NO_2^- concentrations showed not clear trend, NO_3^- concentration at Collier Glacier decreased from supraglacial to glacial outwash to glacial outflow, indicating microbially mediated NO_3^- reduction in the subsurface which is consistent with reducing conditions. DIC concentration also showed an increase from supraglacial to glacial outwash at both Eliot and Collier Glaciers (Fig. 7), consistent with organic carbon being converted to CO_2 and becoming part of the DIC pool in the subglacial system.

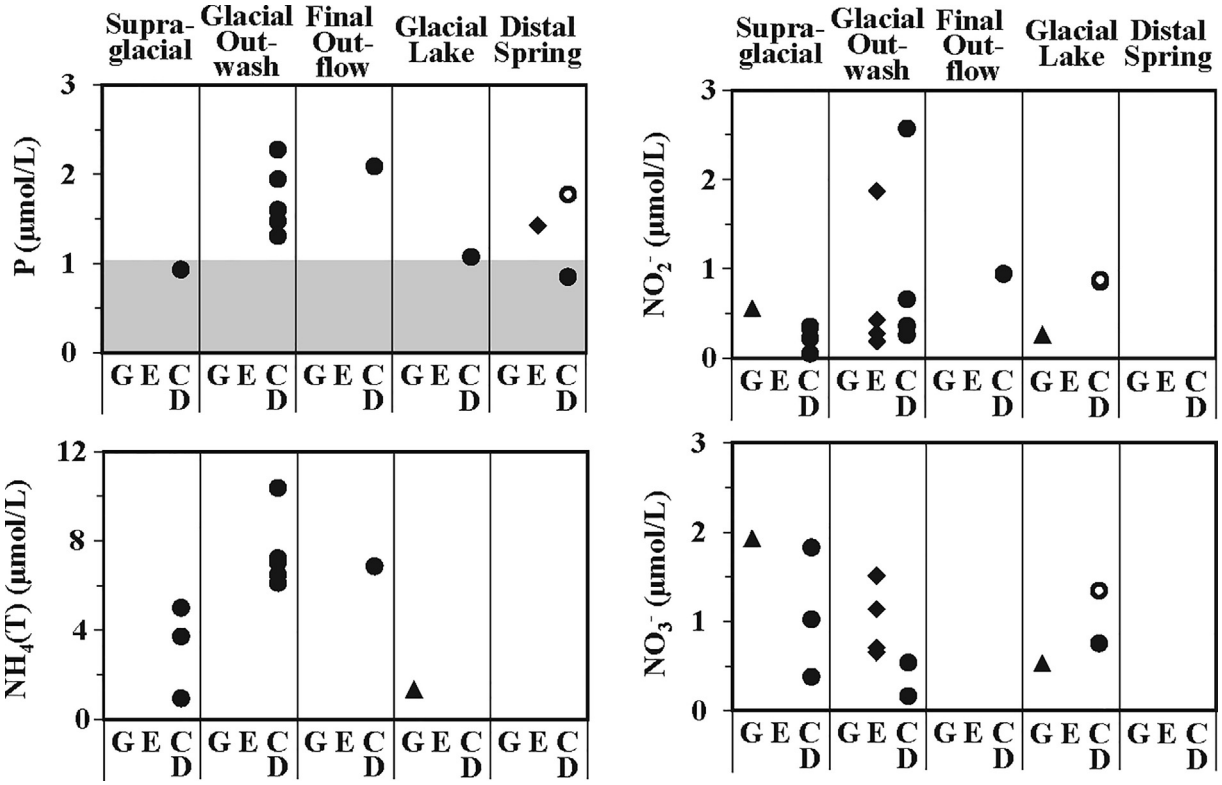

Fig. 6. Total Phosphorous (P, top left), total ammonia (NH_4(T), bottom left), nitrite (NO_2^-, top right), and nitrate (NO_3^-, bottom right) for supraglacial, subglacial, glacial lake, and distal springs. Closed triangles represent samples from Gotchen Glacier (G), closed diamonds samples from Eliot Glacier (E), closed circles samples from Collier Glacier (C), and open circles samples from Diller Glacier (D). Grey shows field blank value ranges (no field blanks collected for spectrophotometric analyses).

Across all sites there was a general trend of increasing dissolved silica concentration with increasing water-rock interaction, with the lowest concentrations (equal to background levels) recovered from supraglacial sites, and higher concentrations recovered from glacial outwash, final outflow, and glacial lake sites, and the highest concentrations recovered from distal springs (Fig. 7). The increase by about an order of magnitude from supraglacial sites to glacial outwash, but then relatively little change between glacial outwash, final outflow, and glacial lake sites at Collier Glacier suggests chemical weathering happens rapidly in the subglacial system and then reaches a steady state with respect to dissolved silica, consistent with indicators of silica precipitation occurring in the subglacial system as reported by Rutledge et al. (2018) at Collier Glacier. Distal spring sites returned the highest dissolved silica concentrations, as well as the highest DIC concentrations, indicating greater carbonic acid input and subsequent silicate weathering in the subsurface further down the volcanic flanks. Calcium concentration followed the 'stepwise' increases from supraglacial sites with the lowest concentrations, glacial outwash, final outwash, and glacial lakes with intermediate concentrations, and distal springs the highest concentrations. Calcium concentration increases are likely tied to carbonic acid weathering of plagioclase feldspar and/or volcanic glass with intermediate to mafic composition.

Contrary to the stepwise increase in concentration observed in dissolved silica, DIC, and calcium, trace element concentration for Al, Fe, and Ti exhibited a different pattern. At Collier Glacier, Al, Fe, and Ti all followed the pattern of low concentration at supraglacial sites to high concentration in the glacial outwash sites, the highest concentration recovered from the final outflow site, and then concentrations decreasing to lake sites, and distal spring sites recovering concentrations similar to supraglacial sites. This is consistent with highest rates of silicate mineral dissolution from chemical weathering happening immediately in the subglacial environment, but suggests liberated trace elements may be sequestered locally proximal to the glacier and not transported downstream.

4.5. Microbially-mediated weathering in volcanically-hosted glaciers

Glacial systems can be treated as weathering drivers that contain two primary microbial community reservoirs (Fig. 8). The accumulation of snow generating flowing glacial ice acts to pulverize and comminute rock, and the pressure at the base of a glacier will drive melting, creating an environment with a high water-rock contact surface. On the surface of the glacier cold-adapted phototrophs (in the case of these study sites it was algae, though cold-adapted cyanobacteria can also be present) colonize the

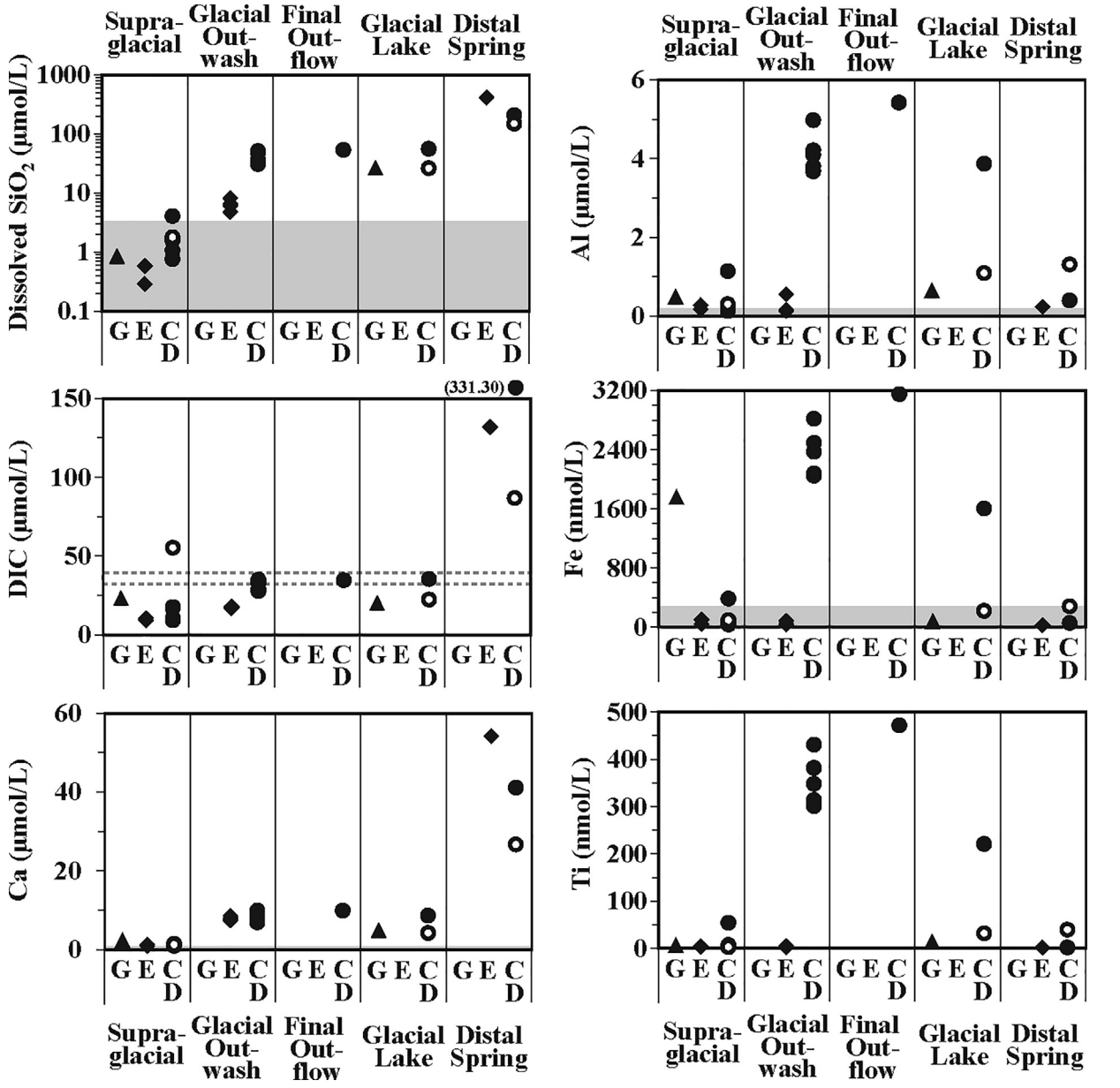

Fig. 7. Aqueous Geochemistry of dissolved SiO_2 (top left), dissolved inorganic carbon (DIC, middle left), Ca (lower left), Al (top right), Fe (middle right), and Ti (bottom right) for supraglacial, subglacial, glacial lake, and distal springs. Closed triangles represent samples from Gotchen Glacier (G), closed diamonds samples from Eliot Glacier (E), closed circles samples from Collier Glacier (C), and open circles samples from Diller Glacier (D). Grey shows field blank value ranges. Dashed lines show range of DI field blanks for DIC. Note that dissolved silica is plotted logarithmically, while all other elements are linear scales. Concentration values for DIC and Ca are from this study and data previously reported (Rutledge et al., 2018), as indicated in Tables 3a and 3b.

snow and ice, fixing CO_2 into organic carbon and converting excess sunlight into heat to drive local melting and provide liquid water for the algae (Dial et al., 2018). Eukaryotic snow algae are dependent upon delivery of fixed nitrogen to the glacier surface (as well as P and trace elements from aeolian deposition of rock and soil particles; Psenner, 1999; Hodson et al., 2005; Stibal et al., 2009), while cyanobacteria inhabiting supraglacial environments have the capacity for biological nitrogen fixation, alleviating that need (Englund and Meyerson, 1974; Christner et al., 2003; Stibal et al., 2006; Edwards et al., 2011; Telling et al., 2011). Processing and cycling of C and N occur on the glacial surface and living and dead cells (as C_{org}, containing P and fixed N, as well as fixed carbon) and cellular byproducts (such as respired CO_2 as DIC, NO_3^-, and organic molecules as DOC and C_{org}) can be washed into crevasses and cracks that act as conduits for water from the supraglacial environment to be transported to the subglacial environment. In the subglacial environment any oxidants are consumed with the breakdown of

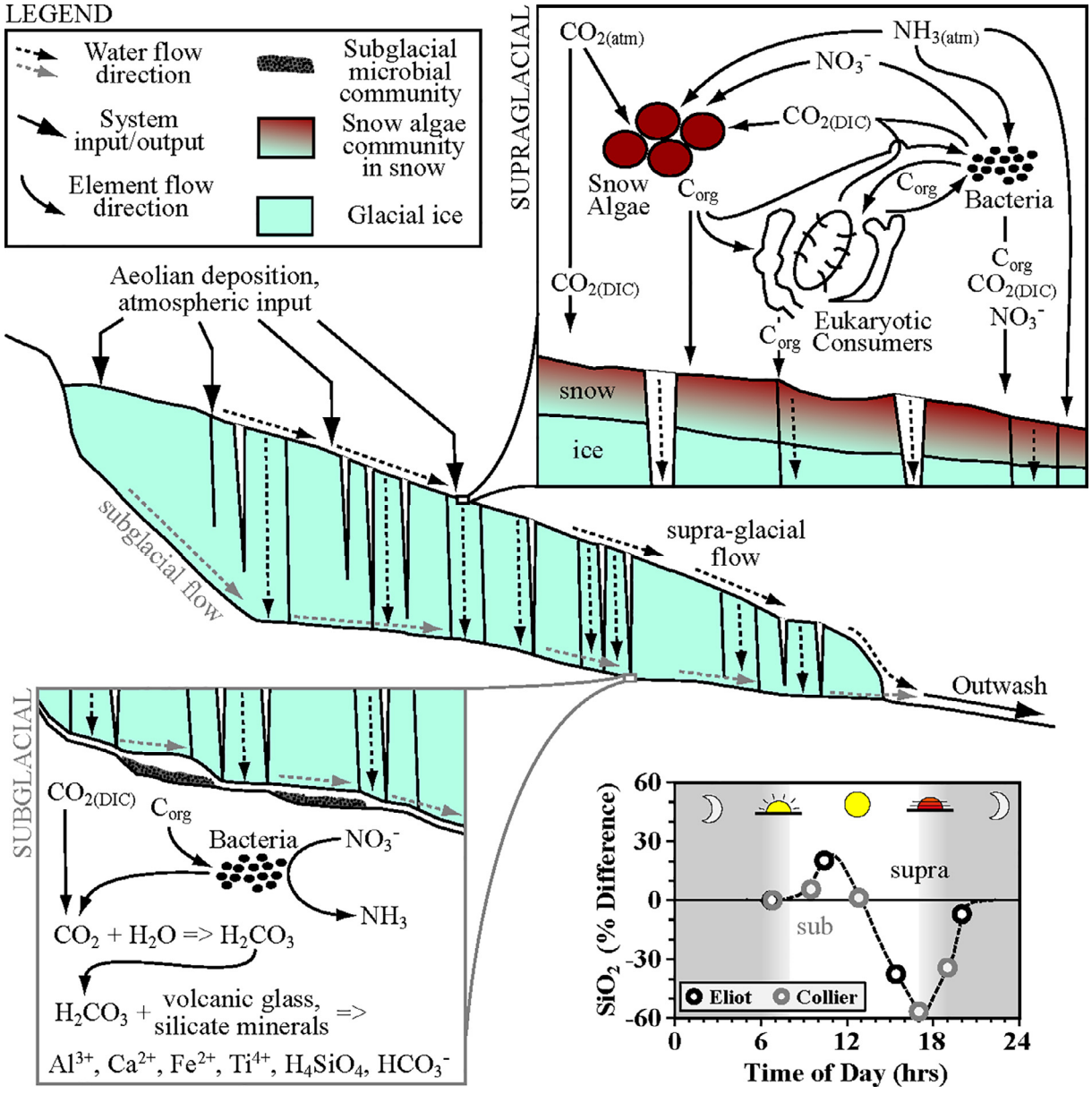

Fig. 8. Conceptual Model. CO_2, fixed N (as NH_3) and P from aeolian deposition are taken up and cycled by snow algae microbial communities, with supraglacially-sourced microbial biomass/C_{org} transported to the subsurface and feeding subglacial heterotrophs, generating CO_2 locally. Carbonic acid weathering in the subglacial system breaks down silicate minerals and volcanic glass, leading to generation of dissolved solutes (SiO_2, Fe, Al, Ti, etc.), as well as release of P and reduction and release of ammonia during breakdown of organic material. Comparison of the percent difference in outwash dissolved silica concentration reveals a diurnal cycle driven by daily melt regimes during the summer: Subglacial flow is dominant from after the sun is no longer shining on the surface and surface melt ends through to early in the morning after sunlight hits the glacial surface and drives supraglacial melt, leading to flushing of low flow (high silica concentration) water followed by dominance of high flow (low silica concentration) water. Short subglacial residence times highlight the potential importance of daily inputs of organic carbon from supraglacial snow algae community sources for subglacial microbial communities in driving weathering reactions.

organic carbon, and CO_2 is generated, producing carbonic acid (H_2CO_3). The carbonic acid then reacts with the comminuted rock, driving weathering and dissolution of silicate minerals and volcanic glass and releasing trace elements, silica, and bicarbonate, as well as generating dissolved phosphorous and ammonia. All of these dissolution and breakdown products are then transported via basal flow to the outwash, with subglacial water sometimes reaching the supraglacial environment before the outwash. The outwash then serves as the mechanism for delivery of generated products to streams/rivers/the ocean. Supraglacial flow is driven by daily warming, with freezing temperatures at night shutting down flow while subglacial flow is driven by pressure. Thus, daily (and seasonal) temperature fluctu-

ations give overall glacial outwash a pulse (Fig. 8), with daytime production of biomass and water feeding subsurface microbial communities (and thus driving weathering) on a diurnal and seasonal cycle. C_{org} fixed by supraglacial phototrophic communities and transported to the subsurface, then, acts as a direct feeder of subglacial heterotrophic microbial communities, with resulting C_{org}-derived CO_2 available to drive chemical weathering of subglacial rock above and beyond weathering driven by DIC delivered from the surface. As an example, the relative changes in dissolved silica concentrations through the daily melt-freeze cycle at Eliot and Collier Glaciers show the highest concentration occurs associated with slower-flowing discharge at night which is then flushed out and replaced by supraglacial melt (carrying organic carbon from the surface) during the day (Fig. 8). These results are consistent with previous work that suggests a connection between supraglacial environments and subglacial microbial communities in alpine glacial settings (Fountain and Walder, 1998; Fountain et al., 2005; Hodson et al., 2008; Laybourn-Parry et al., 2012; Hotaling et al., 2017).

5. CONCLUSIONS

The more they are studied, the more it is shown that rather than cold deserts that inhibit life, glacial surfaces are in fact teaming with microbial life generating biomass via photosynthesis and driving weathering processes on the surface and in the subsurface. In this study, glacial systems in the Pacific Northwest were selected to better understand microbial community composition and productivity on glacial systems hosted in volcanic rock. Light-dependent primary productivity was observed across a range of supra- and periglacial sites. The recovery of photoautotrophic algae from sediment samples suggest the niche space for common snow algae genera is not limited to snow surfaces and snow rich in inorganic debris is also host to snow algae as are proximal sediments. Because both snow algae and inorganic debris lower albedo, this co-occurrence could be advantageous due to increased availability of liquid water and nutrients but this hypothesis requires further testing. The recovery of snow algae OTUs from proximal sediments combined with the observation that light-dependent inorganic carbon assimilation occurs in sediments suggests snow algae are active beyond the snow surface but further studies are necessary to confirm if cold, sunlit sediments are also a niche space for snow algae populations. Deposition of fixed nitrogen as ammonia is a crucial nitrogen source for snow algae communities, though some may rely more on input of fixed nitrogen from allochthonous organic material. The transport of fixed carbon as biomass into the subsurface feeds subsurface microbial communities which in turn generate CO_2, producing carbonic acid which drives mineral dissolution at the rock-water-ice interface. These processes are similar to those described for other glacial systems (both alpine and continental) indicating supraglacial life has been a common feature throughout Earth's history. Furthermore, supraglacial photoautotrophs could have played an important role as primary producers during snowball/global glaciation events, stimulated by increasing atmospheric CO_2 and feeding subglacial microbial communities which in turn drive weathering and delivery of nutrients to the oceans. Lastly, given the long history of glaciation events on Earth for the past 2.9 billion years and the fact that life thrives on volcanic rock-hosted glacial systems, supraglacial and subglacial environments may have (and may still) serve as refugia for life on Mars.

ACKNOWLEDGEMENTS

JRH and TLH would like to acknowledge Courtney Motley for her help in sample processing, Jordyn Miller for her help and assistance in field work and sample collection, Helen Rogers for assistance, Dr. Aaron Diefendorf for his generous assistance in analyzing samples, and Robert and Sally Havig for their generous help and use of their garage as a lab during expeditions. JRH would like to acknowledge the University of Cincinnati and the University of Minnesota for financial support. JRH and TLH would also like to thank the National Forest Service for access to Wilderness Areas. JRH and TLH would like to acknowledge the Yakima, Chinook, Wasco and Wishram, and Molalla First Nations peoples, on whose traditional lands this work was conducted (source: Native-Land.ca).

APPENDIX A. SUPPLEMENTARY MATERIAL

Supplementary data to this article can be found online at https://doi.org/10.1016/j.gca.2018.12.024.

REFERENCES

Aciego S. M., Riebe C. S., Hart S. C., Blakowski M. A., Carey C. J., Aarons S. M., Dove N. C., Botthoff J. K., Sims K. W. W. and Aronson E. L. (2017) Dust outpaces bedrock in nutrient supply to montane forest ecosystems. *Nat. Comm.* **8**, 14800.

Albertsen M., Karst S. M., Ziegler A. S., Kirkegaard R. H. and Nielsen P. H. (2015) Back to basics - the influence of DNA extraction and primer choice on phylogenetic analysis of activated sludge communities. *PLoS One* **10**, e0132783.

Anesio A. M. and Laybourn-Parry J. (2012) Glaciers and ice sheets as a biome. *Trends Ecol. Evol.* **27**(4), 219–225.

Apprill A., McNally S., Parsons R. and Weber L. (2015) Minor revision to V4 region SSU rRNA 806R gene primer greatly increases detection of SAR11 bacterioplankton. *Aq. Microb. Ecol.* **75**(2), 129–137.

Bernhardt H., Hiesinger H., Reiss D., Ivanov M. and Erkeling G. (2013) Putative eskers and new insights into glacio-fluvial depositional settings in southern Argyre Planitia, Mars. *Planet. Space Sci.* **85**, 261–278.

Boyd E. S., Hamilton T. L., Havig J. R., Skidmore M. and Shock E. S. (2014) Chemolithotrophic primary production in a subglacial ecosystem 6146–6153. *Appl. Environ. Microbiol.* **80**. https://doi.org/10.1128/AEM.01956-14.

Boyd E. S., Lange R. K., Mitchell A. C., Havig J. R., Hamilton T. L., Shock E. L., Peters J. W. and Skidmore M. (2011) Diversity, abundance, and potential activity of nitrifying and denitrifying microbial assemblages in a subglacial ecosystem. *Appl. Environ. Microbiol.* **77**(4), 4778–4787. https://doi.org/10.1128/AEM.00376-11.

Caporaso J. G., Lauber C. L., Walters W. A., Berg-Lyons D., Huntley J., Fierer N., Owens S. M., Betley J., Fraser L., Bauer M. and Gormley N. (2012) Ultra-high-throughput microbial

community analysis on the Illumina HiSeq and MiSeq platforms. *ISME J.* **6**(8), 1621.

Christner B. C., Kvitko B. H. and Reeve J. N. (2003) Molecular identification of bacteria and eukarya inhabiting an Antarctic cryoconite hole. *Extremophiles* **7**, 177–183.

Comeau A. M., Li W. K., Tremblay J. É., Carmack E. C. and Lovejoy C. (2011) Arctic Ocean microbial community structure before and after the 2007 record sea ice minimum. *PloS One* **6** (11).

Dhariwal A., Chong J., Habib S., King I., Agellon L. B. and Xia J. (2017) MicrobiomeAnalyst - a web-based tool for comprehensive statistical, visual and meta-analysis of microbiome data. *Nuc. Acids Res.* **45**, W180–W188.

Deng Y., Li Y. and Li L. (2018) Experimental investigation of nitrogen isotopic effects associated with ammonia degassing at 0–70 °C. *Geochim. Cosmochim. Acta* **226**, 182–191.

Dial R. J., Becker M., Hope A. G., Dial C. R., Thomas J., Slobodenko K. A., Golden T. S. and Shain D. H. (2016) The role of temperature in the distribution of the glacier ice worm, *Mesenchytraeus solifugus* (Annelida: Oligochaeta: Enchytraeidae). *Arctic, Antarctic, Alpine Res.* **48**(1), 199–211.

Dial R. J., Ganey G. Q. and Skiles S. M. (2018) What color should glacier algae be? An ecological role for red carbon in the cryosphere. *FEMS Microb. Ecol.* **94**(3). https://doi.org/10.1093/femsec/fiy007.

Edgar R. C., Haas B. J., Clemente J. C., Quince C. and Knight R. (2011) UCHIME improves sensitivity and speed of chimera detection. *Bioinformatics* **27**, 2194–2200. https://doi.org/10.1093/bioinformatics/btr381.

Edwards J. S. (1985) How small ectotherms thrive in the cold without really trying. *Cryo-Letters* **6**, 338–390.

Edwards A., Anesio A. M., Rassner S. M., Sattler B., Hubbard B. P., Perkins W. T., Young M. and Griffith G. W. (2011) Possible interactions between bacterial diversity, microbial activity and supraglacial hydrology of cryoconite holes in Svalbard. *ISME J.* **5**, 150–160. https://doi.org/10.1038/ismej.2010.100.

Englund B. and Meyerson H. (1974) In situ measurement of nitrogen fixation at low temperatures. *Oikos*, 283–287.

Fairchild I. J. and Kennedy M. J. (2007) Neoproterozoic glaciation in the Earth System. *J. Geol. Soc.* **164**(5), 895–921.

Foght J., Aislabie J., Turner S., Brown C. E., Ryburn J., Saul D. J. and Lawson W. (2004) Culturable bacteria in subglacial sediments and ice from two southern hemisphere glaciers. *Microb. Ecol.* **47**(4), 329–340.

Fountain A. G., Jacobel R. W., Schlichting R. and Jansson P. (2005) Fractures as the main pathways of water flow in temperate glaciers. *Nature* **433**, 618–621.

Fountain A. G. and Walder J. S. (1998) Water flow through temperate glaciers. *Rev. Geophys.* **36**, 299–328.

Freyer H. D. (1978) Seasonal trends of NH4+ and NO3− nitrogen isotope composition in rain collected at Jülich, Germany. *Tellus* **30**(1), 83–92.

Fujii M., Takano Y., Kojima H., Hoshino T., Tanaka R. and Fukui M. (2010) Microbial community structure, pigment composition, and nitrogen source of red snow in Antarctica. *Microb. Ecol.* **59**(3), 466–475.

Gohl D. M., Vangay P., Garbe J., MacLean A., Hauge A., Becker A., Gould T. J., Clayton J. B., Johnson T. J. and Hunter R. (2016) Systematic improvement of amplicon marker gene methods for increased accuracy in microbiome studies. *Nature* **201**, 6.

Goodman D. (1971) Ecological Investigations of Ice Worms on Casement Glacier, Southeastern Alaska. Columbus: Ohio State University Research Foundation, Institute of Polar Studies Report No. 39.

Grzesiak J., Zdanowski M. K., Górniak D., Świątecki A., Aleksandrzak-Piekarczyk T., Szatraj K., Sasin-Kurowska J. and Nieckarz M. (2015) Microbial community changes along the Ecology Glacier ablation zone (King George Island, Antarctica). *Polar Biol.* **38**(12), 2069–2083.

Gumsley A. P., Chamberlain K. R., Bleeker W., Söderlund U., de Kock M. O., Larsson E. R. and Bekker A. (2017) Timing and tempo of the Great Oxidation Event. *PNAS* **114**(8), 1811–1816.

Hamilton T. L. and Havig J. R. (2017) Primary productivity of snow algae communities on stratovolcanoes of the Pacific Northwest. *Geobiology*. https://doi.org/10.1111/gbi.12219.

Hamilton T. L. and Havig J. R. (2018) Inorganic carbon addition stimulates snow algae primary productivity. *ISME J.* **1**. https://doi.org/10.1038/s41396-018-0048-6.

Hamilton T. L., Peters J. W., Skidmore M. L. and Boyd E. S. (2013) Molecular evidence for an active endogenous microbiome beneath glacial ice. *ISME J.* **7**(7), 1402.

Hartzell P. L., Nghiem J. V., Richio K. J. and Shain D. H. (2005) Distribution and phylogeny of glacier ice worms (*Mesenchytraeus solifugus* and *Mesenchytraeus solifugus rainierensis*). *Can. J. Zool.* **83**, 1206–1213.

Head J. W., Neukum G., Jaumann R., Hiesinger H., Hauber E., Carr M., Masson P., Foing B., Hoffmann H., Kreslavsky M. and Werner S. (2005) Tropical to mid-latitude snow and ice accumulation, flow and glaciation on Mars. *Nature* **434**(7031), 346.

Hisakawa N., Quistad S. D., Hester E. R., Martynova D., Maughan H., Sala E., Gavrilo M. V. and Rohwer F. (2015) Metagenomic and satellite analyses of red snow in the Russian Arctic. *PeerJ* **3**, e1491.

Hodač L., Hallmann C., Spitzer K., Elster J., Faßhauer F., Brinkmann N., Lepka D., Diwan V. and Friedl T. (2016) Widespread green algae Chlorella and Stichococcus exhibit polar-temperate and tropical-temperate biogeography. *FEMS Microbiol. Ecol.* **92**(8).

Hodson A., Anesio A. M., Tranter M., Fountain A., Osborn M., Priscu J., Laybourn-Parry J. and Sattler B. (2008) Glacial ecosystems. *Ecol. Monogr.* **78**, 41–67.

Hodson A. J., Mumford P. N., Kohler J. and Wynn P. M. (2005) The High Arctic glacial ecosystem: new insights from nutrient budgets. *Biogeochemistry* **72**(2), 233–256.

Holtgrieve G. W., Schindler D. E., Hobbs W. O., Leavitt P. R., Ward E. J., Bunting L., Chen G., Finney B. P., Gregory-Eaves I., Holmgren S. and Lisac M. J. (2011) A coherent signature of anthropogenic nitrogen deposition to remote watersheds of the northern hemisphere. *Science* **334**(6062), 1545–1548.

Hoham R. W. and Duval B. (2001) Microbial ecology of snow and freshwater ice with emphasis on snow algae. In *Snow ecology: an interdisciplinary examination of snow-covered ecosystems* (eds. H. G. Jones, J. W. Pomeroy, D. A. Walker and R. W. Hoham). Cambridge University Press, Cambridge, UK, pp. 168–228.

Hotaling S., Hood E. and Hamilton T. L. (2017) Microbial ecology of the alpine cryosphere: glaciers, subglacial environments, and meltwater streams. *Environ. Microbiol.* **19**, 2935–2948. https://doi.org/10.1111/1462-2920.13766.

Hristov A. N., Zaman S., Vander Pol M., Ndegwa P., Campbell L. and Silva S. (2009) Nitrogen losses from dairy manure estimated through nitrogen mass balance and chemical markers. *J. Environ. Qual.* **38**(6), 2438–2448.

Jickells T. D., Kelly S. D., Baker A. R., Biswas K., Dennis P. F., Spokes L. J., Witt M. and Yeatman S. G. (2003) Isotopic evidence for a marine ammonia source. *Geophys. Res. Let.* **30** (7).

Kargel J. S. and Strom R. G. (1992) Ancient glaciation on Mars. *Geology* **20**(1), 3–7.

Kopp R. E., Kirschvink J. L., Hilburn I. A. and Nash C. Z. (2005) The Paleoproterozoic snowball Earth: a climate disaster triggered by the evolution of oxygenic photosynthesis. *PNAS* **102** (32), 11131–11136.

Kozich J. J., Westcott S. L., Baxter N. T., Highlander S. K. and Schloss P. D. (2013) Development of a dual-index sequencing strategy and curation pipeline for analyzing amplicon sequence data on the MiSeq Illumina sequencing platform. *Appl. Environ. Microbiol.* **79**, 5112–5120. https://doi.org/10.1128/AEM.01043-13.

Laybourn-Parry J., Tranter M. and Hodson A. J. (2012) *The Ecology of Snow and Ice Environments*. Oxford University Press, Oxford, UK.

Lillquist K. and Walker K. (2006) Historical glacier and climate fluctuations at Mount Hood, Oregon. *Arctic, Antarctic, Alpine Res.* **38**(3), 399–412.

Lutz S., Anesio A. M., Jorge Villar S. E. and Benning L. G. (2014) Variations of algal communities cause darkening of a Greenland glacier. *FEMS Microb. Ecol.* **89**(2), 402–414.

Lutz S., Anesio A. M., Edwards A. and Benning L. G. (2015) Microbial diversity on Icelandic glaciers and ice caps. *Front. Microbiol.* **6**, 307.

Lutz S., Anesio A. M., Edwards A. and Benning L. G. (2017) Linking microbial diversity and functionality of arctic glacial surface habitats. *Environ. Microbiol.* **19**(2), 551–565.

Lutz S., Anesio A. M., Raiswell R., Edwards A., Newton R. J., Gill F. and Benning L. G. (2016) The biogeography of red snow microbiomes and their role in melting arctic glaciers. *Nat. Comm.* **7**, 11968.

Macko S. A. and Ostrom N. E. (1994) Pollution studies using stable isotopes. In *Stable Isotopes in Ecology and Environmental Science* (eds. K. Lajtha and R. H. Michener). Blackwell, Boston, pp. 45–62.

Madeleine J. B., Forget F., Head J. W., Levrard B., Montmessin F. and Millour E. (2009) Amazonian northern mid-latitude glaciation on Mars: a proposed climate scenario. *Icarus* **203** (2), 390–405.

Maritz J. M., Rogers K. H., Rock T. M., Liu N., Joseph S., Land K. M. and Carlton J. M. (2017) An 18S rRNA workflow for characterizing protists in sewage, with a focus on zoonotic trichomonads. *Microb. Ecol.* **74**(4), 923–926.

McMurdie P. J. and Holmes S. (2013) phyloseq: an R package for reproducible interactive analysis and graphics of microbiome census data. *PloS one* **8**(4), e61217.

Melezhik V. A. (2006) Multiple causes of Earth's earliest global glaciation. *Terra Nova* **18**(2), 130–137.

Mitchell A. C., Lafrenière M. J., Skidmore M. L. and Boyd E. S. (2013) Influence of bedrock mineral composition on microbial diversity in a subglacial environment. *Geology* **41**(8), 855–858.

Mook W. G., Bommerson J. C. and Staverman W. H. (1974) Carbon isotope fractionation between dissolved bicarbonate and gaseous carbon dioxide. *Earth Planet. Sci. Let.* **22**(2), 169–176.

Musilova M., Tranter M., Bamber J. L., Takeuchi N. and Anesio A. M. (2016) Experimental evidence that microbial activity lowers the albedo of glaciers. *Geochem. Perspect. Lett.* **2**, 106–116.

Nolin A. W., Phillippe J., Jefferson A. and Lewis S. L. (2010) Present-day and future contributions of glacier runoff to summertime flows in a Pacific Northwest watershed: Implications for water resources. *Water Resour. Res.* **46**(12).

Oksanen J. F., Blanchet G., Friendly M., Kindt R., Legendre P., McGlinn D., Minchin P. R., O'Hara R. B., Simpson G. L., Solymos P., Stevens M. H. H., Szoecs E., and Wagner Helene (2018) vegan: Community Ecology Package. R package version 2.5-3. https://CRAN.R-project.org/package=vegan.

Pelto M. S. (2010) Forecasting temperate alpine glacier survival from accumulation zone observations. *The Cryosphere* **4**(1), 67–75.

Psenner R. (1999) Living in a dusty world: airborne dust as a key factor for alpine lakes. *Water, Air, Soil Pol.* **112**(3–4), 217–227.

Peura S., Bertilsson S., Jones R. I. and Eiler A. (2015) Resistant microbial co-occurrence patterns inferred by network topology. *Appl. Environ. Microbiol.*, AEM-03660.

R Core Team (2017) *R: A Language and Environment for Statistical Computing*. R Foundation for Statistical Computing, Vienna, Austria https://www.R-project.org/.

Ramirez R. M. and Craddock R. A. (2018) The geological and climatological case for a warmer and wetter early Mars. *Nat. Geosc.* **11**(4), 230.

Rasmussen B., Bekker A. and Fletcher I. R. (2013) Correlation of Paleoproterozoic glaciations based on U-Pb zircon ages for tuff beds in the Transvaal and Huronian Supergroups. *Earth Planet. Sci. Let.* **382**, 173–180.

Remias D., Holzinger A. and Lütz C. (2009) Physiology, ultrastructure and habitat of the ice alga *Mesotaenium berggrenii* (Zygnemaphyceae, Chlorophyta) from glaciers in the European Alps. *Phycologia* **48**(4), 302–312.

Remias D., Pichrtová M., Pangratz M., Lütz C. and Holzinger A. (2016) Ecophysiology, secondary pigments and ultrastructure of Chlainomonas sp. (Chlorophyta) from the European Alps compared with Chlamydomonas nivalis forming red snow. *FEMS Microbiol. Ecol.* **92**(4).

Royer D. L., Berner R. A., Montañez I. P., Tabor N. J. and Beerling D. J. (2004) CO_2 as a primary driver of phanerozoic climate. *GSA Today* **14**(3), 4–10.

Rutledge A. M., Horgan B. H. N., Havig J. R., Rampe E. B., Scudder N. A. and Hamilton T. L. (2018) Silica dissolution and precipitation in glaciated volcanic environments and implications for Mars. *Geophys. Res. Let.* **45**. https://doi.org/10.1029/2018GL078105.

Schloss P. D., Westcott S. L., Ryabin T., Hall J. R., Hartmann M., Hollister E. B., Lesniewski R. A., Oakley B. B., Parks D. H., Robinson C. J. and Sahl J. W. (2009) Introducing mothur: open-source, platform-independent, community-supported software for describing and comparing microbial communities. *Appl. Environ. Microbiol.* **75**(23), 7537–7541.

Schmidt S. K., Lynch R. C., King A. J., Karki D., Robeson M. S., Nagy L., Williams M. W., Mitter M. S. and Freeman K. R. (2010) Phylogeography of microbial phototrophs in the dry valleys of the high Himalayas and Antarctica. *Proc. Royal Soc. B: Biol. Sci.* **278**(1706), 702–708.

Segawa T., Ishii S., Ohte N., Akiyoshi A., Yamada A., Maruyama F., Li Z., Hongoh Y. and Takeuchi N. (2014) The nitrogen cycle in cryoconites: naturally occurring nitrification-denitrification granules on a glacier. *Environ. Microbiol.* **16**(10), 3250–3262.

Segawa T., Takeuchi N., Fujita K., Aizen V. B., Willerslev E. and Yonezawa T. (2018) Demographic analysis of cyanobacteria based on the mutation rates estimated from an ancient ice core. *Heredity* **120**(6), 562.

Sharp M., Parkes J., Cragg B., Fairchild I. J., Lamb H. and Tranter M. (1999) Widespread bacterial populations at glacier beds and their relationship to rock weathering and carbon cycling. *Geology* **27**(2), 107–110.

Stibal M., Anesio A. M., Blues C. J. D. and Tranter M. (2009) Phosphatase activity and organic phosphorus turnover on a high Arctic glacier. *Biogeoscience* **6**(5), 913–922.

Stibal M., Šabacká M. and Kaštovská K. (2006) Microbial communities on glacier surfaces in Svalbard: impact of physical and chemical properties on abundance and structure of

cyanobacteria and algae. *Microbial Ecol.* **52**(4), 644. https://doi.org/10.1007/s00248-006-9083-3.

Stoeck T., Bass D., Nebel M., Christen R., Jones M. D., Breiner H. W. and Richards T. A. (2010) Multiple marker parallel tag environmental DNA sequencing reveals a highly complex eukaryotic community in marine anoxic water. *Mol. Ecol.* **19** (1), 21–31.

Symonds R. B., Poreda R. J., Evans W. C., Janik C. J., and Ritchie B. E. (2003) Mantle and crustal sources of carbon, nitrogen, and noble gases in Cascade-Range and Aleutian-Arc volcanic gases. USGS Open-File Report, 03-436.

Takeuchi N. (2013) Seasonal and altitudinal variations in snow algal communities on an Alaskan glacier (Gulkana glacier in the Alaska range). *Environ. Re. Lett.* **8**(3), 035002.

Takeuchi N. and Kohshima S. (2004) A Snow Algal Community on Tyndall Glacier in the Southern Patagonia Icefield, Chile. *Arctic, Antarctic, Alpine Res.* **36**(1), 92–99.

Tanaka S., Takeuchi N., Miyairi M., Fujisawa Y., Kadota T., Shirakawa T., Kusaka R., Takahashi S., Enomoto H., Ohata T. and Yabuki H. (2016) Snow algal communities on glaciers in the Suntar-Khayata Mountain Range in eastern Siberia, Russia. *Polar Sci.* **10**(3), 227–238.

Telling J., Anesio A. M., Tranter M., Irvine-Fynn T., Hodson A., Butler C. and Wadham J. (2011) Nitrogen fixation on Arctic glaciers, Svalbard. *J. Geophys. Res.: Biogeosci.* **116**(3).

Telling J., Boyd E. S., Bone N., Jones E., Tranter M. J. L., MacFarlane M. P., Wadham J., LaMarche-Gagnon G., Skidmore M. L., Hamilton T. L., Hill E., Jackson M. and Hodgson D. A. (2015) Rock comminution as a source of hydrogen for subglacial ecosystems. *Nat. Geosci.* **8**, 851–855. https://doi.org/10.1038/ngeo2533.

Terashima M., Umezawa K., Mori S., Kojima H. and Fukui M. (2017) Microbial community analysis of colored snow from an Alpine Snowfield in Northern Japan reveals the prevalence of betaproteobacteria with snow algae. *Front. Microbiol.* **8**, 1481.

Tynen M. J. (1970) The geographical distribution of ice worms (O1igochaeta: Enchytraeidae). *Canad. J. Zool.* **48**(6), 1363–1367.

Uetake J., Naganuma T., Hebsgaard M. B., Kanda H. and Kohshima S. (2010) Communities of algae and cyanobacteria on glaciers in west Greenland. *Polar Sci.* **4**(1), 71–80.

Wolfe A. P., Van Gorp A. C. and Baron J. S. (2003) Recent ecological and biogeochemical changes in alpine lakes of Rocky Mountain National Park (Colorado, USA): a response to anthropogenic nitrogen deposition. *Geobiology* **1**(2), 153–168.

Wynn P. M., Hodson A. and Heaton T. (2006) Chemical and isotopic switching within the subglacial environment of a High Arctic glacier. *Biogeochemistry* **78**(2), 173–193.

Yallop M. L., Anesio A. M., Perkins R. G., Cook J., Telling J., Fagan D., MacFarlane J., Stibal M., Barker G., Bellas C. and Hodson A. (2012) Photophysiology and albedo-changing potential of the ice algal community on the surface of the Greenland ice sheet. *ISME J.* **6**(12), 2302.

Yoshimura Y., Kohshima S. and Ohtani S. (1997) A community of snow algae on a Himalayan glacier: change of Algal biomass and community structure with altitude. *Arctic Alpine Res.* **29**(1), 126–137.

Young G. M., Brunn V. V., Gold D. J. and Minter W. E. L. (1998) Earth's oldest reported glaciation: physical and chemical evidence from the Archean Mozaan Group (~ 2.9 Ga) of South Africa. *J. Geol.* **106**(5), 523–538.

Associate editor: Josef P. Werne